REPORT DOCUMENTATION PAGE	Form Approved OMB No. 0704-0188

1. AGENCY USE ONLY *(Leave blank)*	2. REPORT DATE	3. REPORT TYPE AND DATES COVERED
	11.Jan.99	THESIS

4. TITLE AND SUBTITLE
THE USE OF SATELLITE MICROWAVE RAINFALL MEASUREMENTS TO PREDICT EASTERN NORTH PACIFIC TROPICAL CYCLONE INTENSITY

5. FUNDING NUMBERS

6. AUTHOR(S)
CAPT WEST DEREK A

7. PERFORMING ORGANIZATION NAME(S) AND ADDRESS(ES)
OHIO STATE UNIVERSITY

8. PERFORMING ORGANIZATION REPORT NUMBER

9. SPONSORING/MONITORING AGENCY NAME(S) AND ADDRESS(ES)
THE DEPARTMENT OF THE AIR FORCE
AFIT/CIA, BLDG 125
2950 P STREET
WPAFB OH 45433

10. SPONSORING/MONITORING AGENCY REPORT NUMBER
FY99-71

11. SUPPLEMENTARY NOTES

12a. DISTRIBUTION AVAILABILITY STATEMENT
Unlimited distribution
In Accordance With AFI 35-205/AFIT Sup 1

12b. DISTRIBUTION CODE

13. ABSTRACT *(Maximum 200 words)*

14. SUBJECT TERMS	15. NUMBER OF PAGES
	78
	16. PRICE CODE

17. SECURITY CLASSIFICATION OF REPORT	18. SECURITY CLASSIFICATION OF THIS PAGE	19. SECURITY CLASSIFICATION OF ABSTRACT	20. LIMITATION OF ABSTRACT

Standard Form 298 (Rev. 2-89) (EG)
Prescribed by ANSI Std. 239.18
Designed using Perform Pro, WHS/DIOR, Oct 94

THE USE OF SATELLITE MICROWAVE RAINFALL MEASUREMENTS TO PREDICT EASTERN NORTH PACIFIC TROPICAL CYCLONE INTENSITY

DISSERTATION PROPOSAL

By

Derek A. West, M.S.

* * * * *

The Ohio State University

1997

Proposed Doctoral Committee:

Dr. Jay Hobgood, Adviser

Dr. John Rayner

Dr. Jeffery Rogers

Dr. Carolyn Merry

Atmospheric Sciences Graduate Program

ABSTRACT

This proposed study examines the potential use of satellite passive microwave rainfall measurements derived from Special Sensor Microwave/Imager (SSM/I) radiometers onboard the Defense Meteorological Satellite Program (DMSP) constellation to improve eastern North Pacific Ocean tropical cyclone intensity change forecasting techniques. Relationships between parameters obtained from an operational SSM/I-based rainfall measuring algorithm and 12-, 24-, 36-, 48-, 60- and 72-hour intensity changes from best track data records are examined in an effort to identify statistically significant predictors of intensity change.

Correlations between rainfall parameters and intensity change are analyzed using tropical cyclone data from three years, 1992 to 1994. Stratifications based upon tropical cyclone intensity, rate of intensity change, climatology, translation, landfall and synoptic-scale environmental forcing variables are studied to understand factors that may affect a statistical relationship between rainfall parameters and intensity change. The predictive skill of statistically significant rainfall parameters is assessed by using independent tropical cyclone data from another year, 1995. In addition, case studies on individual tropical cyclones are conducted to gain insight on predictive performance and operational implementation issues.

Impacts of these statistically significant rainfall parameters on a multiple linear regression-based, eastern North Pacific tropical cyclone intensity change forecasting method under development by Hobgood and Petty at The Ohio State University are studied. The overall goal is to determine if SSM/I rainfall parameters can add predictive skill to an objective, intensity change guidance product. The guidance product's skill in predicting intensity change is assessed by statistically comparing its 12-, 24-, 36-, 48-, 60- and 72-hour intensity change forecast errors with those from official National Hurricane Center forecasts, simple persistence and no change.

ACKNOWLEDGMENTS

I wish to thank my adviser, Dr. Jay Hobgood, for intellectual support, encouragement and enthusiasm which made this dissertation proposal possible and for his patience in correcting both my stylistic and scientific errors. Members of my proposed doctoral committee (i.e., Dr. John Rayner, Dr. Jeffery Rogers and Dr. Carolyn Merry) provided constructive criticism of my research efforts. Many thanks go out to my fellow graduate students and friends. Mr. Kevin Petty, Mr. Kenneth Yetzer, Mr. Chung-Chieh Wang, Mr. Maurice McHugh and others gave many hours of help, support and insightful discussion. Department of Geography computer support technicians Mr. James DeGrand, Mr. Sang-Ki Hong and Mr. Jens Bledvad aided my research efforts. Special thanks go to those that helped me obtain PV~WAVE software to conduct data display and analysis (i.e., Dr. Larry Brown and Mr. Geoff Hulse). Mr. John Snowden of the Center for Mapping helped with understanding the use of 8 mm tape drives.

The United States Air Force gave me the opportunity to conduct this research via an assignment to the Air Force Institute of Technology Civilian Institutions (AFIT/CI) Program. My research efforts were aided tremendously by the professional staff of the Air Weather Service Technical Library (AWSTL). The AWSTL staff (i.e., Mr. Charles Travers, Mr. David Pigors, SSgt Tosha French and Mr. Gary Swanson) provided me with

hard to obtain reference materials crucial to this research. Mr. Tom Ross and Ms. Debbie Wolfe of the Air Force Combat Climatology Center (AFCCC, OL-A) co-located at the National Climatic Data Center (NCDC) in Asheville, North Carolina provided me with important data. Also, I would like to thank the staff of the inter-library loan office at The Ohio State University for helping me to obtain relevant references.

Naval Research Laboratory personnel in Monterey, California provided a great deal of guidance and a software program (TROPX) during this research. Mr. Jeffery Hawkins, Dr. Joseph Turk, Mr. Kim Richardson, Mr. Charles "Buck" Sampson and Mr. Thomas Lee all went out of their way to assist me. Mr. Don Boucher and Ms. Arlene Kishi (Hughes Aerospace Corporation), Dr. Mark DeMaria and Dr. Steve Lyons (NHC), Major Roger Edson (JTWC), Lieutenant Colonel Joel Martin (HQ AWS), Lieutenant Paul McCrone (AFGWC), Mr. Frank Wells (JTWC), Dr. Russell Elsberry (NPS), Dr. Grant Petty (PU), Dr. Marie Colton (FNMOC) and Mr. Ralph Ferraro (NESDIS) provided excellent advice. Marshall Space Flight Center (DAAC) in Huntsville, Alabama provided me with SSM/I data. Colonel Judd Staley (OFCM), Ms. Nancy Everson (NESDIS), Dr. K. Abe (WMO), Dr. William Gray and Mrs. Barbara Brumit (CSU), Mr. Gerald Felde (AFGL/PLH), Dr. Marja Bister (MIT) and Mr. Gene Poe and Glenn Sandlin (NRL-DC) provided me very useful reference materials.

VITA

January 3, 1969	Born - Macon, Georgia
1991	B.S., Psychology, United States Air Force Academy, Colorado
1993	M.S., Atmospheric Sciences, The Ohio State University
1993-1995	Officer-in-Charge, Special Operations Weather Team, 16th Special Operations Wing, Hurlburt Field, Florida
1995-present	Captain, Air Force Institute of Technology with duty at The Ohio State University

FIELDS OF STUDY

Major Field: Atmospheric Sciences

TABLE OF CONTENTS

Page

LIST OF TABLES

LIST OF FIGURES

CHAPTER 1

INTRODUCTION

1.1 Defining the Problem

Predictions of tropical cyclone movement and intensity are two "critical" forecast problems (Simpson and Riehl 1981). Currently, intensity forecasting is the operational tropical cyclone forecaster's "greatest problem" requiring the development of effective objective guidance (Gross and Lawrence 1996). This research proposes to examine this important problem with an emphasis on improving tropical cyclone intensity prediction in the eastern North Pacific Ocean basin.

Before going further, some of the relevant terms should be defined. A tropical cyclone is a warm-core, nonfrontal low pressure system of synoptic scale that develops over tropical or subtropical waters and has a definite organized surface circulation (OFCM 1996). This study's basin of interest is the Pacific Ocean west of Central America and Mexico, east of 140 degrees West longitude, north of the Equator and generally south of 35 degrees North latitude (OFCM 1996). As the World Meteorological Organization (WMO) Regional Specialized Meteorological Center (RSMC) for Regional Association IV (RA IV), the National Hurricane Center (NHC) of

the Tropical Prediction Center (TPC) in Miami, Florida, is responsible for issuing forecast and warning advisories for tropical cyclones in the eastern North Pacific (Neumann 1993).

Intensity refers to the one minute average maximum low-level sustained wind speed of the tropical cyclone (Holland 1993). Tropical cyclones in the eastern North Pacific are classified according to their intensity into the following categories. Tropical depressions have intensities less than 17 m s^{-1}, tropical storm intensities are between 17 m s^{-1} and 32 m s^{-1} and a hurricane's intensity is greater than or equal to 33 m s^{-1} (OFCM 1996). With relevant terms defined, attention can be turned to the specific research problem.

Department of Defense (DoD) research into the operational prediction of tropical cyclone intensity can be traced back to the United States Navy's Project AROWA (Applied Research; Operational Weather Analyses). Professor Herbert Riehl, University of Chicago, spearheaded research on this project. In 1951, Project AROWA was tasked to develop techniques to allow, "The prediction of storm intensities and the extent of areas dangerous to surface ships and aircraft along the path of the tropical cyclone" (US Navy 1956). Progress toward the goal of predicting tropical cyclone intensity change has proven to be slow and difficult (OFCM 1997; AMS 1993). Dr. Robert Sheets (1990), former NHC director, summarized current intensity change prediction skill as, "sorely lacking." Research interest in this topic continues to the present and is the source of much debate (Elsberry *et al.* 1992).

Despite producing the highest frequency of tropical cyclones per unit area on the globe (McBride 1995), the eastern North Pacific is perhaps the least studied tropical cyclone basin (Tai and Ogura 1987). This unfortunate situation is most likely due to a scarcity of conventional meteorological observations. However, the lack of data does not diminish a critical need for accurate intensity forecasts which impact several agencies. Only recently has research been directed at understanding the specific processes affecting tropical cyclone intensity in the eastern North Pacific by Whitney and Hobgood (1997) at The Ohio State University. Their research focused on the relationship between climatological sea surface temperatures (SST) and maximum potential intensities (MPI) of tropical cyclones in this region.

1.2 Those Impacted by the Problem

With nearly 6500 km of coastline, a growing tourism industry and a fleet of fishing vessels threatened by the devastating impacts of eastern North Pacific tropical cyclones, the Mexican government requires accurate intensity forecasts to properly allocate a finite amount of resources to the associated preparation and response efforts. Commercial shipping transiting the region with destinations west of the Panama Canal are often directly impacted by tropical cyclones.

DoD operations in the basin include the US Navy's Third Fleet based out of San Diego, California, and Pacific Air Forces headquartered in Hawaii. Naval forecasters are required to make intensity forecasts out to 72 hours to support Optimum Track Ship Routing (OTSR) operations (Titley 1995). An incorrect intensity forecast can create a

potentially dangerous situation for ships. At a recent Interdepartmental Hurricane Conference, one of the US Navy's senior forecasters stressed the importance of intensity forecasts to naval commanders and the urgent need for improved accuracy of intensity forecasts out to at least 72 hours (Barbor 1997). Forecasters at the Air Force Global Weather Center (AFGWC) Americas Region Forecast Branch also have responsibilities to support DoD operations in the eastern North Pacific.

1.3 Application of Satellite Remote Sensing to the Problem

Budgetary constraints prevent the operational use of manned aerial reconnaissance to collect *in situ* measurements from tropical cyclones in this basin. Only on rare occasions are research flights conducted in the eastern North Pacific (OFCM 1997). Therefore, meteorological satellites have become the main source of data for the operational specification and prediction of tropical cyclone intensity (Dvorak 1990) in this otherwise data sparse region. During a recent panel discussion, Mr. Charles "Chip" Guard, University of Guam, suggested remotely sensed rainfall measurements might lead to advances in intensity forecasting skill (Elsberry *et al.* 1992).

Three regions of the electromagnetic spectrum are operationally employed in attempts to estimate rainfall from satellites. These regions are visible (i.e., $\lambda \approx 0.4$ to 0.7 μm), infrared (i.e., $\lambda \approx 10.6$ to 12.6 μm) and microwave (i.e., $\lambda \approx 0.3$ to 3.0 cm). Of these spectral regions, only satellite techniques using microwave measurements can produce physically direct estimates of rainfall (Barrett and Beaumont 1994). This proposed study will examine the potential use of satellite passive microwave rainfall

measurements derived from Special Sensor Microwave/Imager (SSM/I) radiometers (Hollinger 1991) onboard the Defense Meteorological Satellite Program (DMSP) constellation to improve eastern North Pacific tropical cyclone intensity forecasting techniques. Relationships between parameters obtained from an operational SSM/I-based rainfall measuring algorithm (Ferraro *et al.* 1996) and 12-, 24-, 36-, 48-, 60- and 72-hour intensity changes from postanalysis determined best track data records are examined in an effort to identify statistically significant predictors of intensity change.

Latent heat released by condensation in rainfall is recognized as an important factor in tropical cyclone intensity change. Previous studies using SSM/I data show correlations between rain rate or latent heat release and intensity trends in western North Pacific (Rodgers and Pierce 1995a; Rao and MacArthur 1994) and Atlantic (Rodgers *et al.* 1994b) tropical cyclones. In this proposed study, correlations between rainfall parameters within a 444.4 km radius of the center and intensity change are analyzed using eastern North Pacific tropical cyclone data from three years, 1992 to 1994. Stratifications based upon tropical cyclone intensity, rate of intensity change, climatology, translation, landfall and synoptic-scale environmental parameters are studied to understand factors that may affect a statistical relationship between rainfall parameters and intensity change. The predictive skill of statistically significant rainfall parameters is assessed by using independent tropical cyclone data from another year, 1995.

1.4 Goals of this Research

The overall goal is to determine if SSM/I rainfall parameters can add predictive skill to an objective, intensity change guidance product under development by Hobgood (1997) and Petty (1997) at The Ohio State University. The resulting guidance product's skill in predicting intensity change is assessed by statistically comparing its 12-, 24-, 36-, 48-, 60- and 72-hour intensity change forecast errors with those from official NHC, simple persistence and no change forecast techniques. Specific goals related to the research problem are now defined. Goals listed below are classified as primary or secondary. They serve as benchmarks for conducting this research and are directly linked to the data and methodology used to achieve them. Those goals listed as secondary will be fully explored as time permits.

1.4.1 Primary Goal 1

Determine if correlations between rainfall parameters derived from an operational algorithm and eastern North Pacific tropical cyclone future 12- to 72-hour intensity changes from best track data are statistically significant at the 0.95 level. That is, a rainfall parameter will be considered a statistically significant predictor of intensity change if the probability that the correlation coefficient is different from zero is greater than 0.95.

1.4.2 Primary Goal 2

Examine rainfall parameter and intensity change correlations based upon stratifications in current intensity, rate of intensity change, month, location, SST, environmental vertical shear of the horizontal wind, translation speed and landfall.

1.4.3 Primary Goal 3

If rainfall parameters are significantly correlated with intensity change, attempt to include them, via step-wise multiple linear regression, into an intensity change prediction model for eastern North Pacific tropical cyclones already composed of climatology, geography, persistence (Hobgood 1997) and synoptic-scale environmental predictors (Petty 1997). Statistical significance level will be 0.95 for entry into the prediction model and 0.90 to remain.

1.4.4 Primary Goal 4

If rainfall parameters remain in the regression-based model, statistically compare the 12- to 72-hour intensity change prediction errors produced by the resulting model with those errors produced by official NHC, Hobgood (1997), Petty (1997), simple persistence and no change forecast techniques. The statistical significance of differences in errors will be assessed by performing paired *t* tests at the 0.95 level. Success for rainfall parameters improving intensity change forecasts is defined as the final model producing smaller intensity change forecast errors than the methods of Hobgood (1997) and Petty (1997). Also, the final model's intensity forecast errors will be compared against the other methods according to stratifications in current intensity and rate of intensity change.

1.4.5 Primary Goal 5

Conduct case studies on individual tropical cyclones to assess forecast model skill and demonstrate operational implementation issues. Number of case studies conducted will be determined by the time available for this research.

1.4.6 Primary Goal 6

Determine if rainfall parameters can detect the concentric eyewall cycle described by Willoughby *et al.* (1982) and Willoughby (1990). The concentric eyewall cycle is a temporal evolution of convective rings that often occurs in tropical cyclones. The cycle has an important impact on tropical cyclone intensity change.

1.4.7 Secondary Goal 1

Document the rainfall characteristics for a substantial sample of eastern North Pacific tropical cyclones with respect to tropical cyclone intensity, rate of intensity change and radial distance from the center of circulation. This has never been done in the eastern North Pacific.

1.4.8 Secondary Goal 2

Analyze the errors in locating tropical cyclone centers of circulation with SSM/I data. Stratify error analysis by tropical cyclone intensity.

1.4.9 Secondary Goal 3

Attempt to detect a diurnal cycle in eastern North Pacific tropical cyclone rainfall. Examine the possible relationship between tropical cyclone intensity and such a cycle, if a cycle is detected.

1.4.10 Secondary Goal 4

Demonstrate the stability of climatology, geography, persistence and synoptic-scale environmental variables as predictors of eastern North Pacific tropical cyclone intensity change. This will be done by statistical analysis of a dependent data set from different tropical cyclone seasons than those seasons used by Hobgood (1997) and Petty

(1997). Stable intensity change predictors should have similar correlation coefficients for different tropical cyclone seasons.

1.4.11 Secondary Goal 5

Contribute to the Naval Research Laboratory Marine Meteorology Division's efforts to develop a neural network-based tropical cyclone intensity specification technique (Hawkins *et al.* 1996) by processing SSM/I data with adequate coverage of tropical cyclones in the eastern North Pacific.

1.4.12 Secondary Goal 6

Present the findings of this research in a scholarly journal or DoD technical report, at appropriate technical conferences and in electronic format on the Internet.

1.5 Summary

The research problem and associated terms were defined and specific goals were enumerated above. The main hypothesis underlying this proposed research is that satellite passive microwave measured rainfall, through its concomitant latent heat release, will be highly correlated with tropical cyclone intensity changes out to 72 hours in the future. These strong correlations will be useful in improving objective guidance tools for the critical forecasting problem of predicting tropical cyclone intensity changes in the eastern North Pacific. Chapters to follow will provide information on previous research relevant to this proposal, specific information on the data available and tools to be used to achieve the stated goals. A final chapter will discuss accomplishments completed to date related to this proposed research.

CHAPTER 2

RELEVANT LITERATURE REVIEW

2.1 Current State of Tropical Cyclone Intensity Forecasting in the Eastern North Pacific

Improvement of intensity forecasting is rated as a "high" priority research objective by federal agencies involved with tropical cyclone research (OFCM 1997). Table 1 demonstrates the current intensity forecasting skill for the eastern North Pacific during two time periods of interest.

Mean Absolute Official NHC Intensity Forecast Errors for Eastern North Pacific										
Time Period	12 hours		24 hours		36 hours		48 hours		72 hours	
	$m\ s^{-1}$	knots	$m\ s^{-1}$	knots	$m\ s^{-1}$	knots	$m\ s^{-1}$	knots	$m\ s^{-1}$	knots
1988-1993[a]	--	--	3	6	--	--	9	17	10	20
1990-1994[b]	4	7	6	12	8	16	10	19	11	22

Table 1: Mean Absolute Official NHC Intensity Forecast Errors ([a]OFCM 1997; [b]Gross and Lawrence 1996).

Care should be taken when viewing Table 1, because it demonstrates mean absolute

forecast errors. The errors for individual tropical cyclones can be quite large, especially for tropical cyclones that undergo unexpected rapid intensity changes. Improvement in understanding and predicting intensity change in the eastern North Pacific is needed.

2.2 Role of Latent Heat Release in Intensity Change

In 1835, Professor James Pollard Espy proclaimed that the release of latent heat due to the condensation of water vapor into precipitation (e.g., rainfall) plays a major role in tropical cyclones (Middleton 1965). Thus, the foundation for a convection or thermal theory of tropical cyclones was laid (Khrgian 1959). Numerical modeling and observational studies have shown that latent heat release is the most important diabatic process driving tropical cyclones (Anthes 1974). Latent heat release generates available potential energy in the form of a warm-core, low pressure center that may be converted into kinetic energy. The conversion to kinetic energy occurs when friction causes low-level winds to accelerate inward toward the tropical cyclone center. Additionally, this conversion is most effective within about 555.5 km of the center. Therefore, tropical cyclone intensity is highly sensitive to changes in latent heat release (i.e., condensation) within this region.

Figure 1 illustrates the interaction of the synoptic-scale water and motion fields in a tropical cyclone. Moisture (i.e., water vapor) and liquid water (i.e., cloud liquid water and precipitation) and horizontal and vertical motion are linked in a complicated, nonlinear manner via latent heat release (Atlas and Thiele 1981). A tangible indication of the amount of condensation occurring in a tropical cyclone is precipitation (i.e., rainfall).

If properly measured, rainfall can provide useful information for understanding the link between latent heat release and tropical cyclone intensity change.

2.3 Satellite Passive Microwave Measurements of Rainfall

Visible and infrared satellite rainfall estimation methods are based upon cloud top temperatures. This is because clouds, even very thin cirrus, are opaque in the visible and infrared spectral regions. By contrast, cloud droplets weakly interact with microwave electromagnetic radiation. However, precipitation strongly affects microwave radiation. Therefore, rainfall can be readily sensed by satellite-based passive microwave radiometers in a physically direct manner. In crude terms, microwave methods are able to "look through clouds and see" rainfall occurring below. The complex interactions between microwave radiation and Earth's surface and atmosphere are summarized in Figure 2. Passive microwave radiometers remotely sense the microwave radiation emitted, absorbed, reflected, transmitted and scattered by the Earth-atmosphere system.

The physically direct relationship between microwave radiation and rainfall will now be illustrated. The relationship begins with Planck's Law for the radiance or brightness emitted by a blackbody:

$$B_\nu(T) = \frac{2h\nu^3}{c^2} \frac{1}{e^{\left(\frac{h\nu}{kT}\right)} - 1} \qquad (1)$$

where $B_\nu(T)$ is the blackbody emitted radiance or brightness in units of W m^{-2} sr^{-1}, h is Planck's constant which is $6.6260755 \times 10^{-34}$ J s, ν is frequency measured in units of Hz,

c is the speed of light in a vacuum which is 2.99792458×10^{8} m s^{-1}, k is Boltzmann's constant which is 1.380658×10^{-23} J K^{-1} and T is the absolute temperature with units of K. Throughout the microwave spectrum and troposphere, $\frac{h\nu}{kT} \ll 1$, which allows the following Taylor series approximation: $e^{\left(\frac{h\nu}{kT}\right)} \approx 1 + \frac{h\nu}{kT}$. Substitution into Equation 1 yields:

$$B_{\nu}(T) \approx \frac{2h\nu^{3}}{c^{2}} \frac{1}{1 + \frac{h\nu}{kT} - 1} = \frac{2h\nu^{3}}{c^{2}} \frac{1}{\frac{h\nu}{kT}} = \frac{2\nu^{2}kT}{c^{2}} = \frac{2kT}{\lambda^{2}} \qquad (2)$$

The resulting Equation 2 is termed the Rayleigh-Jeans approximation. The relative error of the approximation is less than 0.002.

Radiance is beneficial for the remote sensing of rainfall because it is conveniently independent of the distance to the rainfall, if the incidence angle and pathlength are constant. With the Rayleigh-Jeans approximation, radiance is directly related to the absolute or kinetic temperature (i.e., available from a thermometer) of a blackbody. Since space-based radiometers measure radiance instead of blackbody temperature and a blackbody is a theoretical construct not experienced in nature, it is useful to compare the radiance of a real emitter or graybody to that of a blackbody:

$$\frac{B'_{\nu}(T)}{B_{\nu}(T)} \approx \frac{\frac{2kT'}{\lambda^{2}}}{\frac{2kT}{\lambda^{2}}} = \frac{T'}{T} = \frac{T_{B}}{T} \equiv \varepsilon_{\nu} \qquad (3)$$

The ratio in Equation 3 quantifies how efficiently a graybody emits microwave radiation as compared to a blackbody with the same absolute temperature. $B'_{\nu}(T)$ is the radiance of

a graybody which is remotely sensed. T' is the absolute temperature a blackbody would have for a radiance of $B'_\nu(T)$. T is again the absolute temperature of the graybody. T_B is defined as the brightness temperature and is related to the absolute temperature, T, by a physical property of the graybody called emissivity or emittance, ε_ν.

$$\tau_\nu \equiv \frac{\textit{transmitted radiance at } \nu}{\textit{incident radiance at } \nu} \tag{4}$$

$$\rho_\nu \equiv \frac{\textit{reflected radiance at } \nu}{\textit{incident radiance at } \nu} \tag{5}$$

$$\alpha_\nu \equiv \frac{\textit{absorbed radiance at } \nu}{\textit{incident radiance at } \nu} \tag{6}$$

Other useful properties in the discussion of microwave radiance are defined in Equations 4 to 6 as transmittance (i.e., τ_ν), reflectance (i.e., ρ_ν) and absorptance (i.e., α_ν). These are related by the following identity due to conservation of energy considerations: $\tau_\nu + \rho_\nu + \alpha_\nu \equiv 1$. Kirchhoff's Law states that in the case of local thermodynamic equilibrium, a valid assumption for the Earth's atmosphere below 100 km, $\alpha_\nu \equiv \varepsilon_\nu$.

An equation describing the transfers of microwave radiation illustrated in Figure 2 can be written in terms of T_B and T. Using the plane-parallel geometry shown in Figure 3 and neglecting scattering, an equation for microwave radiative transfer involving rainfall is derived (Grody 1997; Kidder and Vonder Haar 1995):

$$\cos\theta \frac{dT_B}{dz} = \sigma_a (T - T_B) \tag{7}$$

The volume absorption coefficient, σ_a, has units of m^{-1}. Above the rain layer, $\sigma_a \approx 0\ m^{-1}$. Therefore, integration of Equation 7 is simplified to the depth of the rain layer, D. Also, the integration can be further simplified by assuming that the temperature of the rain layer, T_r, is constant. The incidence angle, θ, is measured from local vertical to the radiometer. Equation 8 below shows that T_B measured at the radiometer can be represented as the sum of the four components shown graphically in Figure 3:

$$T_B \approx T_1 + T_2 + T_3 + T_4 \tag{8}$$

Each term on the right side of Equation 8 is defined below:

$$T_1 = T_s \varepsilon \tau^{\sec\theta} \tag{9}$$

$$T_2 = (1-\varepsilon) T_c \tau^{2\sec\theta} \tag{10}$$

$$T_3 = (1-\varepsilon) T_r (1-\tau^{\sec\theta}) \tau^{\sec\theta} \tag{11}$$

$$T_4 = T_r (1-\tau^{\sec\theta}) \tag{12}$$

T_1 represents the microwave emission by the surface with temperature T_s and transmission through the atmosphere. Cosmic microwave transmission through the atmosphere and reflection at the surface is described by T_2. T_c is the cosmic radiometric temperature which is quite small (i.e., $T_c \approx 2.7$ K). The rain layer's downwelling

microwave emission, transmission through the atmosphere and reflection by the surface is given by T_3. T_4 describes the upwelling microwave emission by the rain layer and transmission through the atmosphere. Transmittance of the rain layer is approximated by: $\tau \approx e^{(-\sigma_a D)}$. Substitution of Equations 9 to 12 into Equation 8 and rearrangement of terms yields:

$$T_B \approx T_s \varepsilon \tau^{\sec\theta} + (1-\varepsilon) T_c \tau^{2\sec\theta} + T_r [1 - \varepsilon \tau^{\sec\theta} - (1-\varepsilon)\tau^{2\sec\theta}] \qquad (13)$$

If the small cosmic term is neglected in Equation 13, the impact of rainfall on T_B can be simply illustrated. For a nonraining atmosphere, $\tau \approx 1$, which means $T_B \approx T_s \varepsilon$. As rain rate increases, σ_a increases, τ approaches 0 and T_B converges to T_r. Therefore, T_B measurements can provide extremely useful information by their response to rainfall.

Some problems confound the otherwise simple relationship between T_B and rainfall. Over water, T_B increases rapidly with rain rate because ε values for water are relatively low (i.e., $\varepsilon \approx 0.5$). Thus, water provides a radiometrically cool background compared to a warm rain layer target. However, ε values over land are relatively high (i.e., $\varepsilon \approx 0.9$). As a result, land is a warm background for a warm rain layer. Therefore, a change in T_B due to rainfall emissions over land is usually too small to detect. Another problem is that T_B depends on the product of $\sigma_a D$. However, rain rate is highly related to σ_a and independent of D. Therefore, the depth of the rain layer, D, needs to be specified in order for T_B measurements to be used for explicitly determining rain rate. Also, σ_a depends not only on rain rate, but cloud liquid water and water vapor, as well. Consequently, cloud liquid water and water vapor information are necessary to perform

calculations of rain rate from measurements of T_B.

By neglecting scattering and cosmic microwave radiation, Equation 13 implies that as rain rate increases, T_B increases to a limit of T_r. However, in reality there is a point at which increasing rain rate actually results in decreasing values of T_B. This is because as rain rate increases, the size of hydrometeors in the rain layer (e.g., very large rain drops, ice, graupel and hail) increases and approaches the wavelength of microwave radiation. Scattering then occurs which obscures emission by the rain layer and surface and allows reflection of extremely cold cosmic microwave radiation off the top of the rain layer into the radiometer's field of view. The resulting reduction in T_B occurs over water and land surfaces.

The previous discussion in this section describes two regimes for satellite passive microwave measurements of rainfall: emission and scattering. Up to a threshold rain rate governed by wavelength, **emission** by rainfall **over water** allows T_B measurements to be used to calculate rain rate. Beyond that threshold rain rate, **scattering** by large hydrometeors permits T_B measurements to be used to infer rain rate **over water and land.** In general, microwave frequencies below 20 GHz are used in emission-based algorithms. At frequencies above 60 GHz, scattering effects are utilized by passive microwave algorithms. Between these frequencies, emission and scattering effects are found. An excellent summary of the current state-of-the-art algorithms developed by researchers to calculate rain rate from passive microwave brightness temperatures was written by Wilheit *et al.* (1994). The algorithm to be used in this proposed research utilizes both emission and scattering regimes to measure rainfall in eastern North Pacific tropical

cyclones. Details of the relevant algorithm and reasons it was selected for this research are discussed below.

2.4 Rainfall Algorithm to be Used in this Research

An important distinction in rainfall types found in tropical cyclones is convective versus stratiform (Houze 1993). Convective precipitation occurs in cumulus and cumulonimbus clouds of the eyewall and convective rain bands. Nimbostratus clouds in tropical cyclones produce stratiform rainfall. Tropical rain rates less than or equal to 1 mm hr^{-1} are mostly stratiform and those greater than 10 mm hr^{-1} are generally convective (Tokay and Short 1996). Rain rates between these two values can be caused by both types of rainfall. However, a threshold between the two types at 6 mm hr^{-1} was proposed by Johnson and Hamilton (1988).

Processes governing convective precipitation take place above the freezing level and are termed "cold cloud." Passive microwave algorithms best suited for this type of precipitation measurement are those that take advantage of the pronounced scattering effects of the resulting precipitation-sized ice particles. The "warm cloud" processes of stratiform rainfall take place at or below the freezing level. Scattering-based algorithms are not useful in this warm cloud regime. However, emission-based algorithms can detect stratiform rainfall over water.

Greater than 90 percent of the rainfall associated with a tropical cyclone occurs within 222.2 km of the center of circulation (Hughes 1952; Riehl 1954). Of this rainfall, approximately 90 percent of the areal coverage within this region is stratiform (Jorgensen

1984). Due to higher rain rates, convective rainfall contributes about 60 percent of the total rainfall (Marks 1990; Jorgensen 1984). Therefore, the measurement of both convective and stratiform rainfall is important to this study.

The rainfall algorithm chosen for this proposed research was developed by the National Environmental Satellite, Data and Information System (NESDIS) Office of Research Applications (ORA). It was developed to determine instantaneous rain rates using brightness temperature, T_B, data from the DMSP SSM/I (Ferraro *et al.* 1996). Specific details concerning DMSP SSM/I data will be provided in Chapter 3. There are two main components of the NESDIS/ORA over water algorithm: scattering and emission. The scattering component relates a scattering index (Grody 1991; Ferraro *et al.* 1994) to rain rates. This scattering index is the difference between the actual vertically polarized brightness temperature at 85.5 GHz and one predicted for a scattering-free atmosphere by using the vertically polarized brightness temperatures at 19.4 and 22.2 GHz. A brightness temperature screening process is used to prevent false rain retrievals (e.g., sea ice). The emission component is calculated by using cloud liquid water values greater than 0.20 mm estimated using the vertically polarized brightness temperatures at 19.4, 22.2 and 37.0 GHz (Weng and Grody 1994). Scattering index and cloud liquid water relationships with rain rate were empirically developed using coincidental ground-based radar rainfall measurements from around the world (Ferraro and Marks 1995). The range of rain rates detected by the algorithm is between 0.2 mm hr^{-1} and 35.0 mm hr^{-1}. Validation of the algorithm found a relative error between SSM/I and radar rain rates of 0.10 to 0.20. Finally, a practical reason for using the NESDIS/ORA algorithm is that it

was selected by the Shared Processing Program Algorithm Research Panel as the SSM/I rainfall algorithm to be operationally implemented by DoD and other federal agencies (Colton and Poe 1994; Ferraro *et al.* 1996). Therefore, this rainfall product is readily available to NHC forecasters via the Shared Processing Program and the Internet.

2.5 Satellite Passive Microwave Measurements Related to Tropical Cyclone Intensity

Links between space-based passive microwave measurements related to precipitation and tropical cyclone intensity have been explored for over 20 years. The first research on this specific topic was conducted by Adler and Rodgers (1977). By examining six observations of western North Pacific tropical cyclone Nora (1972), they found latent heat release (LHR) increased as intensity increased. LHR (in units of W) within a 444.4 km radius of the tropical cyclone center was calculated with a rainfall algorithm using the 19.4 GHz horizontally polarized brightness temperatures measured by the Nimbus-5 Electrically Scanning Microwave Radiometer (ESMR-5).

Rodgers and Adler (1981) later used 71 observations by the ESMR-5 of 21 tropical cyclones during the 1973 to 1975 seasons. 49 of the observations were for 18 western North Pacific tropical cyclones and 22 of the observations were for 3 eastern North Pacific tropical cyclones. A correlation of 0.71, significant at the 0.99 level, was found between LHR within a 444.4 km radius and current intensity. One case study of eastern North Pacific tropical cyclone Doreen (1973) demonstrated their finding that maximum LHR generally occurred one to two days prior to maximum intensity. This

finding confirmed earlier numerical tropical cyclone prediction model results that showed maximum intensity occurred one to three days after maximum LHR (Kurihara and Tuleya 1974; Rosenthal 1978). Of further interest, Rodgers and Adler (1981) found that the three eastern North Pacific tropical cyclones were more compact and had less rainfall than those of the western North Pacific.

Encouraged by the results of Adler and Rodgers (1977) and Rodgers and Adler (1981), Hunter *et al.* (1981) made the first attempt at an objective tropical cyclone intensity forecast guidance tool including microwave brightness temperature data. They employed an eigenvector representation of the ESMR-5 19.4 GHz horizontally polarized brightness temperature images centered on 120 observations of 29 tropical cyclones from the 1973 to 1974 seasons. 25 were tropical cyclones in the western North Pacific and 4 occurred in the eastern North Pacific. By adding ESMR-5 information to climatology, geography and persistence information from the best track data, they were able to increase the explained variance of intensity by 0.07 at the 24-hour forecast period and by 0.16 at the 72-hour forecast period, when compared to using only best track data. Their guidance product based upon best track and ESMR-5 predictors produced mean absolute forecast errors for the 24- and 72-hour periods that were, respectively, 2 and 4 m s^{-1} less than the mean absolute official forecast errors by the Joint Typhoon Warning Center (JTWC) for the same forecast periods and tropical cyclone seasons.

With the launch of the first SSM/I in 1987, routine operational microwave measurements of tropical cyclones from satellites became possible. The first researcher to relate microwave measurements from the SSM/I to tropical cyclone intensity was

Rhudy (1989). He used 23 observations of 12 tropical cyclones in the western North Pacific and Atlantic during 1987 to 1988. LHR within a 444.4 km radius and current intensity had a correlation of 0.62, significant at the 0.99 level. 85.5 GHz vertically polarized brightness temperature differences within a 333.3 km radius yielded correlations of 0.64 and 0.74, significant at the 0.99 level, with current and future 24-hour intensities, respectively.

Relationships between SSM/I-measured rainfall and future 24-hour intensity change were examined for 27 observations of 12 tropical cyclones in the western North Pacific and Atlantic during 1987 to 1988 (MacArthur 1991; Rao *et al.* 1991; Rao and MacArthur 1994). They found a 0.68 correlation, significant at the 0.95 level, between average volumetric rain rate (in units of $mm^3\ hr^{-1}$) within a 222.2 km radius and future 24-hour intensity change. Case studies of western North Pacific tropical cyclones Lynn (1987) and Dinah (1987) yielded extremely high correlations between average volumetric rain rate within a 222.2 km radius and future 24-hour intensity change. The correlation for Lynn's seven observations was 0.97 and Dinah's four observations was 0.99. Overall, they found a differential effect of rainfall on future intensity change due to location of rainfall with respect to the center of circulation. Within a 222.2 km radius from the center, rainfall had a highly positive correlation with future 24-hour intensity change. However, within the annular region between 222.2 to 444.4 km from the center, rainfall had a weakly negative correlation with future 24-hour intensity change. It was noted that if a rain rate maximum occurred outside of the core region (i.e., beyond a 222.2 km radius), short-term weakening of intensity could be expected.

McCoy (1991) used 85.5 GHz vertically polarized brightness temperature differences between regions (i.e., outer-versus-inner and left-versus-right) within a 444.4 km radius to find a 0.61 correlation with future 24-hour intensity change. He also noted that the appearance of convective rain bands beyond 222.2 km from the center usually preceded a weakening of future 24-hour intensity. His study was based on 25 observations of western North Pacific and Atlantic tropical cyclones during 1987 to 1988. In this study, McCoy (1991) was the first researcher to suggest that SSM/I measurements might be able to monitor the convective ring or concentric eyewall cycle discussed by Willoughby *et al.* (1982 and 1984) and Willoughby (1988 and 1990). This convective ring cycle is a spatial and temporal evolution of axisymmetric convective rainfall rings that commonly occurs in symmetric tropical cyclones with intensities greater than or equal to 45 m s^{-1}. Often a single vigorous circular ring of rainfall or an eyewall within a 111.1 km radius will contract inward with a concomitant intensity increase. Sometimes concentric outer convective rings will form between a 111.1 to 222.2 km radius and contract around the existing eyewall. This outer convective ring causes the inner eyewall to dissipate and intensity decreases. As the outer convective ring continues to contract it often supplants the original eyewall and intensity increases when this new eyewall contracts. The entire eyewall cycle normally takes between 12 to 36 hours to complete. Multiple concentric eyewall cycles may occur provided the tropical cyclone does not make landfall, experience excessive environmental wind shear or travel over relatively cold ocean.

Felde and Glass (1991) used the fractional coverage of 85.5 GHz horizontally polarized brightness temperatures less than 220 K within a tropical cyclone-centered circular area with a 55.5 km radius. Their study used 17 observations of 11 western North Pacific tropical cyclones during the 1987 season. The correlation between fractional coverage of intense convection, indicated by depressed 85.5 GHz brightness temperatures, and current intensity was 0.73. Also, the difference between the 19.4 GHz horizontally and vertically polarized brightness temperatures (i.e., an indication of microwave emission by rainfall) within the same 55.5 km radius yielded a 0.77 correlation with current intensity. For nine observations of intensifying tropical cyclones the correlation increased to 0.85 and for eight observations of weakening tropical cyclones the correlation was 0.70. A later study by Glass and Felde (1992) used 25 observations of 19 western North Pacific tropical cyclones during 1987 to 1988. The same 85.5 GHz parameter described above produced a 0.93 correlation with current intensity for 15 intensifying tropical cyclones and a 0.70 correlation for 10 weakening tropical cyclones.

Alliss *et al.* (1992) conducted a case study of Atlantic tropical cyclone Hugo (1989) using nine SSM/I observations. They found SSM/I-derived rainfall parameters calculated for areas within a 444.4 km radius were highly correlated with current intensity. The highest correlation coefficient was 0.93, significant at the 0.99 level. It was suggested that Hugo's intensity changes might be related to the convective ring cycle. In a similar case study of Atlantic tropical cyclone Florence (1988) using five observations, Alliss *et al.* (1993) found the average rain rate (in units of mm hr^{-1}) within a

111.1 km radius had a correlation of 0.93 with current intensity, significant at the 0.98 level. Both of these studies found that as the azimuthally averaged rainfall maximum moved inward, intensity increased.

In a previous study, this author used 17 SSM/I observations of western North Pacific tropical cyclone Freda (1987), climatological sea surface temperature and global numerical weather prediction (NWP) model data to understand the relationships between rainfall, environmental forcing and intensity (West 1993a and b). Changes in LHR preceded changes of intensity by about 12 hours. Moisture flux convergence in the middle troposphere initiated convective rings in the outer core (i.e., within 111.1 to 222.2 km). Interactions with upper-level troughs aided inner core (i.e., within 111.1 km) rainfall, if vertical wind shear was weak. Changes in intensity were related to the convective ring cycle.

A case study of western North Pacific tropical cyclone Flo (1990) using seven SSM/I observations found a correlation of 0.70 between rainfall within a 111.1 km radius and current intensity (Melton 1994). Zhao (1994) used three cases of western North Pacific tropical cyclones from 1992 to relate rainfall parameters to future intensity. She studied a total of 37 SSM/I observations from 21, 7 and 9 observations of tropical cyclones Gay, Elsie and Hunt, respectively. For intensifying tropical cyclones, the correlation between a measure of total (i.e., convective and stratiform) rainfall within a 111.1 km radius and future 12-hour intensity change was 0.71, highly significant at the 0.999 level. A convective rainfall parameter within a 222.2 km radius yielded a 0.63 correlation, significant at the 0.91 level, with future 12-hour intensity change in

weakening tropical cyclones. Zhao (1994) also found the convective ring cycle occurred in these cases and maximum rainfall occurred prior to maximum intensity.

Rodgers *et al.* (1994b) studied 18 North Atlantic tropical cyclones from 1987 to 1989 with 103 SSM/I observations. They found that more intense tropical cyclones had more rainfall. Additionally, correlations between past 12-hour trends in both LHR within a 111.1 km radius and intensity varied according to the current intensity. That is, for tropical depressions the correlation was 0.06, for tropical storms it was -0.27 and for hurricanes it was 0.78, all significant at the 0.99 level. Rodgers and Pierce (1995a) later examined western North Pacific tropical cyclones from 1987 to 1992 with 257 SSM/I observations. For 123 tropical depression observations the correlation between past 12-hour trends in both average rain rate within a 111.1 km radius and intensity was 0.25, for 61 tropical storm observations it was 0.51 and for 73 typhoon observations it was 0.04, all significant at the 0.99 level. Additionally, a diurnal variation of rainfall within a 444.4 km radius was found for weaker tropical cyclones (i.e., less than tropical storm strength). An early morning maximum and an evening minimum were found for these weaker tropical cyclones. For stronger tropical cyclones, especially within the inner core, no significant diurnal variation was found. These findings support the results of a study by Hobgood (1986) that included the diurnal cycle of net radiation at the cloud tops in a numerical tropical cyclone prediction model. Rodgers *et al.* (1994b) and Rodgers and Pierce (1995a) both found that higher rain rates occurred near the center of tropical cyclones and that the spatial and temporal change of azimuthally averaged rainfall demonstrated the convective ring cycle.

Using SSM/I, climatological SST and global NWP model data, Rodgers *et al.* (1994a) and Rodgers and Pierce (1995b) examined case studies of tropical cyclones to understand environmental forcing, rainfall and intensity relationships. Rodgers *et al.* (1994a) used 30 SSM/I observations of 3 Atlantic tropical cyclones during 1989. Tropical cyclone Dean (1989) had 7 observations, Gabrielle had 11 and Hugo had 12. In Rodgers and Pierce (1995), 18 observations of western North Pacific tropical cyclone Bobbie (1992) were used. In both studies and all cases, the convective ring cycle played an important role in intensity change. A convective ring often formed in the outer core (i.e., between 111.1 and 222.2 km radii) and propagated inward. Maximum intensity occurred when the ring reached the inner core (i.e., within 111.1 km of the center). The formation of outer convective rings usually led to short-term weakening. Environmental forcing affects were similar to those found by West (1993a and b). In a recent case study by Rodgers *et al.* (1997), 13 SSM/I observations of LHR within a 55.5 km radius of Atlantic tropical cyclone Opal (1995) were studied to understand the rapid intensity change that occurred. Three convective bursts took place prior to a rapid intensity increase. They proposed that the rapid intensity change was due to the massive amounts of latent heat released by the convective bursts.

Recently, Cecil (1997) related 85.5 GHz brightness temperature-based ice scattering signatures within a 111.1 km radius to future 24-hour intensity for 90 SSM/I observations of western and eastern North Pacific and Atlantic tropical cyclones. The correlation was 0.68 for all basins. For the 17 observations of 6 eastern North Pacific tropical cyclones the correlation improved to 0.89.

Previous studies of satellite microwave measurements of tropical cyclones indicate that parameters related to rainfall are highly correlated with tropical cyclone intensity change. Used in concert with other factors related to tropical cyclone intensity change, SSM/I-derived rainfall parameters ought to aid in the prediction of eastern North Pacific tropical cyclone intensity change.

2.6 Factors Related to Tropical Cyclone Intensity Change

Strong correlations between rainfall parameters and tropical cyclone intensity were shown above. However, there are other factors affecting tropical cyclone intensity change that might confound attempts to develop a predictive tool for intensity change based solely on rainfall parameters. A brief summary of research on these factors is reviewed below. These factors will be used in the stratified statistical analysis discussed in Section 3.10.

The current intensity of a tropical cyclone can affect the relationship between LHR and future intensity change. Studies by Shapiro and Willoughby (1982), Rodgers *et al.* (1994b) and Rodgers and Pierce (1995a) showed that as tropical cyclone intensity increased, the correlation between LHR within the core region and future intensity change became stronger. This increasingly efficient relationship between LHR and intensity change for more intense tropical cyclones was attributed to increasing lower-tropospheric inertial stability.

Rate of intensity change is an important factor in understanding LHR and future intensity change. Rapid intensity changes (i.e., greater than 11 m s^{-1} over a 12-hour

period) are extremely hard to forecast and cause large official intensity change forecast errors (Elsberry *et al.* 1992; Mundell 1990 and 1991; Sampson *et al.* 1995). Mundell (1990 and 1991) found that extremely intense convection, inferred by infrared satellite measurements, within a 666.6 km radius of the tropical cyclone center usually preceded rapid intensification events by 12 hours.

The climatological (i.e., geographical and monthly) variability of tropical cyclone intensity characteristics was first studied by Frank and Jordan (1960). Whitney (1995) and Whitney and Hobgood (1997) conducted such a study using 31 years of data for the eastern North Pacific. In this study, geographical stratifications were north or south of 18 degrees North latitude and east or west of 110 degrees West longitude. Significant geographical and monthly variations of intensity were found.

A necessary, but not sufficient, condition for tropical cyclone formation is a sea surface temperature of at least 26 °C (Palmén 1948). Also, in a study of eastern North Pacific tropical cyclones by Whitney (1995) and Whitney and Hobgood (1997), the maximum potential intensity was directly related to climatological SST.

Weak tropospheric vertical shear of the horizontal wind is another necessary, but not sufficient, condition for tropical cyclone development (Gray 1968). The vector difference of the horizontal wind at 200 and 850 mb is often used to quantify this vertical shear. In a study of western North Pacific tropical cyclones, Zehr (1992) found values of 200 to 850 mb vertical shear greater than 15 m s^{-1} to be excessive and not conducive to tropical cyclone development.

Translation speeds greater than 10 m s^{-1} are not conducive to intensification (Sampson *et al.* 1995). Tropical cyclone landfall has complex interactions with intensity change (Merrill 1987). Therefore, this proposed research will exclude data at landfall.

2.7 Statistical Prediction of Eastern North Pacific Tropical Cyclone Intensity Change

Recently, research at The Ohio State University has been directed at developing statistically based guidance for forecasting intensity change in eastern North Pacific tropical cyclones (Hobgood 1997; Petty 1997). The research by Hobgood (1997) parallels and expands upon similar research in the North Atlantic by Jarvinen and Neumann (1979). Using ten years (i.e., 1982 to 1993) of best track data (see Section 3.1 for details on this type of data) and climatological SST, ten predictors of future intensity change out to 72 hours were identified. These forecast variables are summarized in Table 2. Also shown in Table 2 is the variance of intensity change explained by these variables at each forecast period and the mean absolute forecast errors for a regression model tested against independent best track data from 1994. These errors compare favorably with mean absolute official NHC intensity forecast errors.

Petty's (1997) research adds synoptic-scale environmental forcing information derived from global NWP model data (see Section 3.1 for more details) to the statistical guidance product developed by Hobgood (1997). This research is analogous to and goes beyond that of DeMaria and Kaplan's (1994) study in the North Atlantic. Additionally, Petty (1997) uses real-time, instead of climatological, SST. By combining the predictors

derived from the NWP model and best track data for three years (i.e., 1989 to 1991), he identified a total of 13 predictors of intensity change. His wind shear, thermal, moisture and eddy flux forecast variables are summarized in Table 2. Also shown in Table 2 is the variance of intensity change explained by these variables at each forecast period.

<table>
<tr><th colspan="6">Summary of Eastern North Pacific Tropical Cyclone Intensity Change Forecasting Techniques Under Development at The Ohio State University</th></tr>
<tr><td colspan="6">Climatology, geography and persistence forecast variables identified by Hobgood (1997) in decreasing order of importance:
1. Latitude*; 2. Current intensity*; 3. Previous 12 hour intensity trend*; 4. Longitude; 5. Distance to land calculated with Kaplan (1992); 6. Absolute value of the Julian date minus 237*; 7. Potential intensification calculated by subtracting the current intensity from the maximum potential intensity defined by Whitney and Hobgood (1997); 8. Zonal component of translation; 9. Meridional component of translation; 10. Translation speed*.</td></tr>
<tr><td colspan="6">Forecast Period</td></tr>
<tr><td>12 hour</td><td>24 hour</td><td>36 hour</td><td>48 hour</td><td>60 hour</td><td>72 hour</td></tr>
<tr><td colspan="6">Explained Variance of Intensity Change (r^2) for Hobgood (1997)</td></tr>
<tr><td>0.48</td><td>0.50</td><td>0.53</td><td>0.57</td><td>0.61</td><td>0.63</td></tr>
<tr><td colspan="6">1994 Mean Absolute Forecast Errors ($m\ s^{-1}$) for Hobgood (1997)</td></tr>
<tr><td>3</td><td>6</td><td>8</td><td>10</td><td>11</td><td>11</td></tr>
<tr><td colspan="6">Synoptic-scale wind shear, thermal, moisture and eddy flux forecast variables identified by Petty (1997) in decreasing order of importance:
1. Absolute vertical wind shear between 500 and 850 mb; 2. Previous 24 hour trend of absolute vertical wind shear between 200 and 850 mb; 3. Zonal component of vertical wind shear between 200 and 850 mb; 4. Temperature difference between 500 and 850 mb; 5. Previous 24 hour trend of 700 mb equivalent potential temperature; 6. 200 mb planetary eddy flux convergence at 700 km radius; 7. Relative angular momentum at 850 mb; 8. Equivalent potential temperature difference between 700 and 850 mb.</td></tr>
<tr><td colspan="6">Explained Variance of Intensity Change (r^2) for Petty (1997)</td></tr>
<tr><td>0.60</td><td>0.60</td><td>0.61</td><td>0.65</td><td>0.68</td><td>0.70</td></tr>
</table>

Table 2: Summary of eastern North Pacific tropical cyclone intensity change forecasting techniques under development at The Ohio State University. * indicates the five forecast variables also used by Petty (1997).

CHAPTER 3

DATA AND METHODOLOGY

3.1 NHC Postanalysis Best Track, SST and ECMWF Model Data

Best track data indicating postanalysis determined tropical cyclone positions (0.1 degree increments) and intensities (2.5 m s^{-1} increments) at six-hour intervals during each named tropical cyclone (i.e., only those tropical cyclones that reached tropical storm or hurricane intensity) from 1992 to 1995 was obtained from the NHC (ftp://ftp.nhc.noaa.gov/pub/tracks/tracks.epa). The data format is described by Davis *et al.* (1984). The positions and intensities for most of the tropical cyclones in the best track data were determined by satellite techniques (Dvorak 1990). The errors associated with using the Dvorak intensity specification technique are not specifically known for the eastern North Pacific. However, in a study of North Atlantic tropical cyclones, Gaby *et al.* (1980) found the mean absolute difference (i.e., accuracy) between satellite-derived and *in situ* intensity measurements was 4 m s^{-1} and the mean difference (i.e., bias) was -2 m s^{-1}. Similarly, in a study of western North Pacific tropical cyclones, Martin and Gray (1993) found the accuracy of satellite estimates was 10 m s^{-1} and the bias was 5 m s^{-1}. The intensity errors in the eastern North Pacific best track data are most likely on the

order of the errors found in the studies cited above.

In addition to the best track data, official NHC intensity forecast error data for these tropical cyclones was obtained from the National Climatic Data Center (NCDC) on 3.5 inch computer diskettes in text format.

Climatology, geography and persistence variables are calculated from the best track data in the same manner as Hobgood (1997). The only exception is that the calculation of potential intensity change in this proposed research uses real-time, instead of climatological, SST data. Calculation of MPI uses SST data from operational analyses at the National Centers for Environmental Prediction (NCEP). This SST data is available from a data archive at the Columbia University in binary format (http://ingrid.ldgo.columbia.edu/descriptions/reynoldsweekly.html). The data is optimally interpolated weekly to a one-degree grid. Details concerning this SST data are described by Reynolds and Smith (1994). SST values are extracted and MPI parameters calculated using the same computer programs from Petty's (1997) research.

The European Centre for Medium-Range Weather Forecasts (ECMWF) NWP model data to be used in this research is from the National Center for Atmospheric Research (NCAR) data archive (http://www.scd.ucar.edu/dss/datasets/ds111.2.html). Model data was made available in binary format to the Atmospheric Sciences Program by the Byrd Polar Research Center at The Ohio State University. The model data was optimally interpolated every 12 hours (i.e., 0000 and 1200 UTC) to a 2.5-degree grid with 15 pressure levels. Synoptic-scale environmental forcing predictors identified by Petty (1997) are calculated using the same computer programs used in his research. The use of

ECMWF model data to evaluate environmental forcing of tropical cyclones was previously shown to be useful by Molinari *et al.* (1992), West (1993a and b), Rodgers *et al.* (1994a) and Rodgers and Pierce (1995b).

3.2 DMSP Constellation of Satellites

A series of DMSP satellites (Block 5D-2) have been launched since 1987. These satellites include flight numbers (F-#) F-8, F-9, F-10, F-11, F-12 and F-13. All of these satellites are equipped with an SSM/I except for F-9. The SSM/I on F-12 failed to function properly shortly after launch. In January, 1989, the F-8 experienced a partial failure of its SSM/I and the satellite mission was terminated in August, 1991. Satellites F-10 and F-11 form a two platform constellation for observations of tropical cyclones from 1992 to 1994. The additional launch of F-13 in 1995 created a three SSM/I constellation for the 1995 tropical cyclone season.

Specific information about the orbits of the relevant DMSP satellites is contained in Table 3. DMSP satellite orbits are near-circular, near-polar and sun-synchronous (i.e., the satellite crosses the Equator at the same local time each day). Inclination of the satellite orbital plane is 98.8 degrees from the Equator resulting in a retrograde orbit. The period for an orbit is 102 minutes which yields 14.1 orbits per day. One satellite, F-10, did not reach the desired orbit. Therefore, its Equator crossing time is changing at a substantial rate shown in Table 3. All of the SSM/I-equipped satellites listed in Table 3 are currently functioning properly and within specification limits.

Flight-Number	Launch Date	Equator Crossing Times Upon Launch [Local Standard Time]		Equator Crossing Times as of 1 Jan 97 [Local Standard Time]		Maximum Altitude (km)	Minimum Altitude (km)
		ascend	descend	ascend	descend		
F-10	1 Dec 90	1942	0742	2223	1023	861	726
F-11	28 Nov 91	1702	0502	1854	0654	878	836
F-13	24 Mar 95	1743	0543	1745	0545	877	840

Table 3: DMSP Orbital Characteristics.

3.3 SSM/I Instrument Specifications

The SSM/I is a seven channel, four frequency, linearly polarized, passive microwave radiometer (Hollinger *et al.* 1990). Spectral channels include vertically and horizontally polarized electromagnetic radiation at 19.4, 37.0 and 85.5 GHz. Only vertically polarized radiation is measured at 22.2 GHz. Resolution of the channels is displayed in Table 4 (Hollinger *et al.* 1990; Poe 1997; Bauer and Grody 1995). Absolute accuracy of the SSM/I-measured brightness temperatures is less than 3 K. Intercalibration of the brightness temperatures measured by the F-10, F-11 and F-13 SSM/I's is between 0.1 to 0.5 K (Wentz 1995; Poe 1997; Colton *et al.* 1996).

Channel Information		Spectral Resolution (GHz)	Radiometric Resolution (K)	Spatial Resolution (km)			Sampling Resolution (km)
Center Frequency (GHz)	Polarization			Along-Track	Along-Scan (IFOV)	Along-Scan (EFOV)	
19.4±0.13	Vertical	0.24	≤ 0.50	69	43	70	25.0
19.4±0.13	Horizontal	0.24	≤ 0.48	69	43	70	25.0
22.2±0.13	Vertical	0.24	≤ 0.55	60	40	65	25.0
37.0±0.55	Vertical	0.90	≤ 0.37	37	28	55	25.0
37.0±0.55	Horizontal	0.90	≤ 0.37	37	29	55	25.0
85.5±0.80	Vertical	1.40	≤ 0.58	15	13	14	12.5
85.5±0.80	Horizontal	1.40	≤ 0.57	15	13	14	12.5

Table 4: SSM/I Channel Resolution Information.

SSM/I scanning characteristics and the resulting geometry are portrayed in Figures 4 through 7. The SSM/I is a conically scanning imager with an active scan angle of 102.4 degrees limited by the body of the spacecraft. Depression and look angles of 45 degrees and a nominal orbital altitude of 833 km yield an incidence or zenith angle of 53.1 degrees. The conical scan, active scan angle and orbital altitude result in a ground swath of about 1394 km. The satellite travels with a speed of 6.58 m s^{-1} and the scan period is 1.899 s. Therefore, the satellite ground track is 12.5 km per scan which nearly equals the spatial resolution of the 85.5 GHz channels. At a sampling interval of 4.22 ms, 128 samples are recorded on every clockwise (i.e., left-to-right) scan for the 85.5 GHz channels. The remaining channels are sampled on every other scan at a 8.44 ms interval resulting in 64 samples.

During each scan the SSM/I is calibrated with a cold target (i.e., a mirrored reflection of deep space which has a brightness temperature of about 2.7 K) and a warm target with a radiometric temperature near 300 K obtained by three precision thermistors. The conically scanning nature of the SSM/I yields a constant incidence angle (i.e., 53.1 degrees) and sensor-to-ground distance throughout each scan. This constant incidence angle allows for invariable planes of polarization and a large fixed polarization difference. Also, the constant sensor-to-ground distance results in uniform spatial resolutions and a consistent pathlength along each scan. Therefore, the limb darkening problem common to cross-track scanners is avoided.

3.4 SSM/I-Related Data

Data measured by the SSM/I are stored onboard the satellite until transmitted to ground receiving and processing stations. During initial processing, this raw data is quality controlled. That is, the data are decommutated, deinterleaved, bit-flipped and restructured into properly ordered orbits. Using scan calibration data, satellite ephemeris and attitude corrections, a geolocated antenna temperature file called a Temperature Data Record (TDR) is created containing data from all seven channels. The geolocation (i.e., ground navigation data) accuracy of each SSM/I sample is less than 6 km (Hollinger 1991). A correction for spill-over, cross-polarization coupling and antenna pattern effects caused by the parabolic reflector used in the SSM/I is required. Therefore, an antenna pattern correction is applied to the TDR to produce a brightness temperature, T_B, file called a Sensor Data Record (SDR). Through the use of scientifically developed

algorithms, the SDR can be converted into a file containing geophysical parameter data (e.g., rainfall) called an Environmental Data Record (EDR).

SSM/I TDR data for DMSP satellite flight numbers F-10 and F-11 can be obtained for the 1992 to 1995 tropical cyclone seasons. In addition, F-13 data are available for the 1995 season. It should be noted that due to SSM/I problems on F-8 and F-12 during the period of interest, data from these specific radiometers is not available for this research. The specific SSM/I data set planned for use in this research is maintained by the Naval Research Laboratory in Washington, DC and Stennis Space Center, Mississippi. Unfortunately, it is not a contiguous data set. That is, not all of the SSM/I orbits from 1992 to 1995 are contained in this library.

The available constellation of radiometers virtually assures at least one coincidental SSM/I observation during a tropical cyclone per day (Velden *et al.* 1989). The probability of at least two observations per day is greater than or equal to 0.89. Spatial and temporal coverage characteristics of SSM/I orbits are graphically summarized in Figures 8 through 10.

3.5 Query Data Library for SSM/I Orbits with Coverage of Tropical Cyclones

Using best track tropical cyclone positions as input, a computer program developed by the Naval Research Laboratory in Washington, DC, determined orbits with adequate coincidental coverage. The computer program used radar-tracked DMSP orbital ephemeris and SSM/I scanning characteristics to perform the required calculations. Output of this program was input to a Corel Quattro Pro 7 spreadsheet database. Using

database functions, orbits were selected from those available in the SSM/I library of the Naval Research Laboratory in Washington, DC and Stennis Space Center, Mississippi. In addition, SSM/I orbits of tropical cyclones located west of 140 degrees West longitude and after or near (i.e., within 55.5 km of a coastline) landfall were excluded from consideration. Determinations of distance to landfall were performed using the best track positions and coastline positions as input to a computer program used at the NHC that was developed by Kaplan (1992) based upon previous research by Merrill (1987). Additional cases with corresponding best track intensities less than 15 m s^{-1} (i.e., 30 knots or Dvorak (1990) Current Intensity Number 2.0) were also eliminated. SSM/I-based tropical cyclone center of circulation determinations (see Section 3.7 for more details) are not feasible for these weaker tropical cyclone intensities (Hawkins, personal communication, 1997; Miller, personal communication, 1997).

3.6 Process SSM/I Orbits with Coincidental Coverage of Tropical Cyclones

A computer software system developed by the Naval Research Laboratory called TROPX will be used to process data from SSM/I orbits with coincidental coverage of tropical cyclones. This tropical cyclone satellite data processing system is a component of the Naval Research Laboratory [NRL] Satellite Image Processing System (NSIPS). TROPX contains display and analysis software tools specifically tailored to conduct multispectral satellite remote sensing studies of tropical cyclones (Helveston *et al.* 1996). TROPX interfaces with Precision Visuals~Workstation Analysis and Visualization Environment (PV~WAVE) software produced by Visual Numerics Incorporated. The

combination of TROPX and PV~WAVE allows SSM/I data to be processed from the raw data format found in the Naval Research Laboratory's archive to TDR, SDR and EDR products.

SSM/I data identified as containing coincidental coverage will be extracted from the archive and transferred to a disk storage device attached to a UNIX workstation. Further processing and database functions will be performed by TROPX on the same workstation. TROPX can be controlled locally or remotely using an Internet connection.

3.7 Locate the Tropical Cyclone Center

The 85.5 GHz horizontally polarized channel (i.e., an SDR product) on the SSM/I provides the necessary spatial resolution and radiometric response to accurately determine the center of tropical cyclones (Melton 1994; Zhao 1994; Alliss *et al.* 1993 and 1992; Rappaport 1991; Glass and Felde 1989 and 1990; Rhudy 1989; Velden *et al.* 1989). See Figures 12 and 13 for examples of 85.5 GHz horizontally polarized T_B images created by TROPX that are useful for this task. The latitude and longitude of the center of circulation will be recorded to the nearest 0.1 degree. Along-track scan number, along-scan position number and scan time of the center of circulation will also be recorded. This information and interpolated best track data will be used to assess the accuracy of tropical cyclone center fixes using SSM/I data.

3.8 Determine if SSM/I Coverage is Adequate

Once an accurate tropical cyclone center fix is accomplished, only an orbit with adequate coverage will be further processed from a brightness temperature (i.e., SDR) to a rainfall (i.e., EDR) image. Swath width considerations and bad or missing data can prevent adequate coverage by a coincidental SSM/I orbit. Adequate orbital coverage is defined as at least half coverage over the ocean of a circular area within 444.4 km of a tropical cyclone center 111.1 km or more from land. These criteria ensure adequate rainfall measurements over water and minimize effects due to landfall (Merrill 1987).

3.9 Apply the Operational Rainfall Algorithm

The rainfall algorithm (Ferraro *et al.* 1996) used in this study was selected for two reasons. First, it has the capability to measure both convective and stratiform rainfall over the ocean. Second, it is the current DoD operational rainfall algorithm (Colton and Poe 1994). See Figures 14 and 15 for examples of rain rate images produced by the NESDIS/ORA algorithm using TROPX.

3.10 Examine Rainfall and Intensity Change Correlations

Using Statistical Package for Social Sciences (SPSS) 7.0 Base Statistics software, descriptive statistics and data analysis tools (e.g., scatter-diagrams, histograms and regression) will be generated (Glahn 1985). The average and time tendency of average rainfall parameters for regions within 444.4 km of the tropical cyclone center will be correlated with current intensity, previous 12-hour intensity trend and future 12- to 72-

hour intensity changes calculated from the best track data. Each SSM/I observation will be assigned to the closest best track time interval within six hours of 0000, 0600, 1200 or 1800 Uniform Time Coordinate (UTC). If more than one SSM/I observation corresponds to the same record, the observation closer in time or with better coverage will be used.

Circular regions are designated as inner core (i.e., 0 to 111.1 km), core (i.e., 0 to 222.2 km) and total (i.e., 0 to 444.4 km). Annular regions are the outer core (i.e., 111.1 to 222.2 km) and exterior (i.e., 222.2 to 444.4 km). These regions are depicted in Figure 11. Average rain rates for these regions will be calculated. Ratios and differences of the average rain rates for the above regions will also be calculated. Additionally, the 12- and 24-hour time tendency of the rainfall parameters will be calculated. The resulting number of candidate rainfall parameters is 51. These parameters are summarized in Table 5 below.

Current			12 hour Tendency (Current - 12 hours prior)			24 hour Tendency (Current - 24 hours prior)		
Averages	**Ratios of Averages**	**Differences of Averages**	**Averages**	**Ratios of Averages**	**Differences of Averages**	**Averages**	**Ratios of Averages**	**Differences of Averages**
inner outer core exterior total	inner/outer inner/core inner/exterior inner/total outer/core outer/exterior outer/total core/exterior core/total exterior/total	inner-outer core-exterior	inner outer core exterior total	inner/outer inner/core inner/exterior inner/total outer/core outer/exterior outer/total core/exterior core/total exterior/total	inner-outer core-exterior	inner outer core exterior total	inner/outer inner/core inner/exterior inner/total outer/core outer/exterior outer/total core/exterior core/total exterior/total	inner-outer core-exterior

Table 5: Candidate Rainfall Parameters.

Stratifications will be used to determine possible factors affecting significant rainfall parameter and intensity change correlations. These stratifications include: current intensity, rate of intensity change, month, location, SST, vertical shear of the horizontal wind, translation speed and landfall. Intensity stratifications are tropical depression (i.e., less than 17 m s^{-1}), tropical storm (i.e., 17 to 32 m s^{-1}), hurricane (i.e., 33 to 50 m s^{-1}) or strong hurricane (i.e., greater than 50 m s^{-1}). Rate of intensity change classes are 12-hour change in intensity greater than 11 m s^{-1} (i.e., rapid strengthening), 11 to -11 m s^{-1} (i.e., normal) or less than -11 m s^{-1} (i.e., rapid weakening). Month stratifications are peak of season (i.e., August and September), early season (i.e., before August) and late season (i.e., after September). Location stratifications are north or south of 18 degrees North latitude and east or west of 110 degrees West longitude. SST stratifications are less than 26 °C or greater than or equal to 26 °C. Vertical shear of the zonal component of the horizontal wind between 200 and 850 mb stratifications are weak (i.e., less than 15 m s^{-1}) or strong (i.e., greater than or equal to 15 m s^{-1}). The stratifications for 12-hour average translation speed are slow (i.e., less than or equal to 10 m s^{-1}) or fast (i.e., greater than 10 m s^{-1}). Landfall stratifications are whether or not the tropical cyclone made landfall during its existence.

3.11 Develop Rainfall Parameter and Intensity Change Prediction Model

Those candidate rainfall parameters found to be significantly correlated with intensity changes at the 0.95 level will be rank ordered by correlation as potential predictors for multiple linear regression model development. Rainfall parameters highly

correlated with 12-, 24-, 36-, 48-, 60- and 72-hour intensity changes will be selected for future analysis. Also, selected parameters will be examined to ensure that they are not highly correlated with each other. The selected potential predictors (i.e., independent variables) and dependent variables (i.e., 12- to 72-hour intensity changes) for the model development data set (i.e., 1992 to 1994) will be normalized. That is, all variables will have the development data set mean for that variable subtracted from it and this difference divided by the standard deviation for the development data set. This allows for dimensionless comparison of the resulting regression coefficients between predictors and across dependent variables (i.e., intensity changes for the different forecast time periods). Via the SPSS step-wise multiple linear regression model development tool, a prediction model based upon rainfall parameters will be constructed. The statistical significance level for entry into the regression model will be 0.95 and 0.90 to remain.

3.12 Combine Rainfall Parameters with Hobgood and Petty Prediction Models

To evaluate the impact of rainfall parameters on other intensity change prediction models under development for the eastern North Pacific (Hobgood 1997; Petty 1997), combined multiple linear regression models will be constructed in a similar manner as the rainfall parameter model. Predictors described by Hobgood (1997) will be computed for the six-hour interval best track data records with corresponding rainfall parameters selected using the same model development data set as Section 3.11. Hobgood's (1997) climatology, geography and persistence predictors and rainfall parameter predictors selected in Section 3.11 will be input as predictor candidates into the SPSS multiple

linear regression model development tool in the same manner as described in Section 3.11. To combine the rainfall parameter predictors with Petty's (1997) model, the rainfall parameters must correspond to 0000 or 1200 UTC. Those rainfall parameters derived from F-11 (and F-13) SSM/I orbits will normally be within three hours of either 0000 or 1200 UTC. However, F-10 orbits will generally be closest to 0600 or 1800 UTC. To prevent large data gaps, F-10 rainfall parameter observations can be used for the nearest time interval within six hours of 0000 or 1200 UTC, if a corresponding F-11 observation is missing. Petty's (1997) climatology, persistence and synoptic-scale environmental parameter predictors and rainfall parameter predictors will be used to develop a third multiple linear regression model as described above.

3.13 Evaluate Intensity Change Prediction Models

The skill of the three models developed in Sections 3.11 and 3.12 will be evaluated by examining the intensity change forecast errors they produce on a data set (i.e., 1995) that is independent of the data set used to create the models. Also, the errors will be compared to those produced by the following methods: Hobgood (1997), Petty (1997), official NHC forecasts, simple persistence of the past 12-hour intensity change trend and predicting no change. Two types of forecast errors will be examined for each forecast interval from 12 to 72 hours. Mean intensity change forecast error (i.e., bias in units of m s^{-1}) is the average value of the difference between the forecasted intensity change and the intensity change that actually occurred. Mean absolute intensity change forecast error (i.e., accuracy in units of m s^{-1}) is the average absolute value of the

difference between the forecasted intensity change and the intensity change that actually occurred.

For the regression-based models, the predictor variables for the evaluation data set (i.e., 1995) will be normalized using the mean and standard deviation from the model development data set (i.e., 1992 to 1994). These normalized values will be input to the regression models. The output will be converted from normalized values to intensity changes for comparison purposes. The forecast errors described above will be calculated for all the methods. Both types of forecast errors for each method will be graphically displayed using Quattro Pro. To understand how well each method performs in various situations, forecast errors will also be stratified by current intensity and rate of intensity change categories described in Section 3.10. The statistical significance of differences in errors produced by the different methods will be assessed by performing paired *t* tests at the 0.95 level.

3.14 Conduct Case Studies

Tropical cyclones with particularly good spatial and temporal coverage by SSM/I orbits will be candidates for in-depth case studies. Also, strong hurricanes with maximum intensities greater than 50 m s^{-1} are significant cases that might prove to be insightful upon close examination. Additionally, those cases exhibiting rapid intensity changes or the concentric eyewall cycle could provide interesting examples of forecast model skill and operational implementation issues for challenging situations. Tropical cyclones Tina (1992) and Olivia (1994) were subjects of aerial reconnaissance research

missions and would be excellent candidates for case studies.

3.15 Survey Rainfall Characteristics of Eastern North Pacific Tropical Cyclones

Averages and standard deviations of rain rates for the areas shown in Figure 11 will be computed for the intensity and intensity change categories in Section 3.10. Calculations will use SSM/I observations from 1992 to 1995. These calculations will be further stratified by time of day in an effort to detect a diurnal cycle of rainfall.

3.16 Analyze Tropical Cyclone Center Position Errors Using the SSM/I

The average and standard deviation of the distance errors between SSM/I determined tropical cyclone centers of circulation (see Section 3.7) and interpolated best track locations will be calculated for 1992 to 1995. Errors will be stratified by current intensity categories in Section 3.10.

CHAPTER 4

ACCOMPLISHMENTS AND PRELIMINARY RESULTS

Time Period	Number of tropical cyclones with maximum intensity of tropical storm	Number of tropical cyclones with maximum intensity of hurricane	Total number of tropical cyclones for the time period	Number of tropical cyclones with at least one coincidental SSM/I orbit	Number of coincidental SSM/I orbits identified for further processing
1992[a]	10	14	24	23	207
1993[b]	4	10	14	12	93
1994[c]	8	9	17	6	49
1992-1994	22	33	55	41	349
1995[d]	3	7	10	10	127
1992-1995	25	40	65	51	476
Climatology (1966-1995)[e]	7	9	16	--	---

Table 6: SSM/I coverage of eastern North Pacific tropical cyclones and number of orbits selected for further processing. Climatology values provided for comparison ([a]Lawrence and Rappaport 1994; [b]Avila and Mayfield 1995; [c]Pasch and Mayfield 1996; [d]Avila and Rappaport 1996; [e]Rappaport and Mayfield 1997).

A database of SSM/I orbits with coincidental coverage of eastern North Pacific tropical cyclones has been created for the seasons of 1992 to 1995. 476 orbits have been identified for further processing at the Naval Research Laboratory Marine Meteorology

Division in Monterey, California. The dependent data set (i.e.,1992 to 1994) to be used in model development contains 349 orbits. There are 127 orbits in the independent data set (i.e., 1995) to be used for model evaluation. Information about coincidental coverage of SSM/I orbits selected for further processing is summarized in Table 6 above.

Some of the climatology, geography, persistence and synoptic-scale environmental variables required by the intensity change prediction models of Hobgood (1997) and Petty (1997) have been calculated for 1993 to 1995. The main focus of current research activities is extraction of SSM/I orbits from the archive, processing of the SSM/I data, generation of the 85.5 GHz horizontally polarized T_B images for center fixing, application of the NESDIS/ORA rainfall algorithm and calculation of rainfall parameters. Tasks related to the SSM/I data will require the author to travel to the Naval Research Laboratory in Monterey, California.

It is expected that rainfall parameters will show predictive skill in determining intensity change and aid efforts to develop a better objective guidance product for the intensity prediction problem. A summary of this proposed research was recently presented by the author at the 22nd Conference on Hurricanes and Tropical Meteorology sponsored by the American Meteorological Society (West 1997). The author expects to defend his dissertation by the Summer of 1998.

LIST OF REFERENCES

Adler, R.F., and E.B. Rodgers, 1977: Satellite-observed latent heat release in a tropical cyclone. *Mon. Wea. Rev.*, **105**, 956-963.

Alliss, R.J., G.D. Sandlin, S.W. Chang, and S. Raman, 1993: Applications of SSM/I data in the analysis of Hurricane Florence (1988). *J. Appl. Meteor.*, **32**, 1581-1591.

-----, S. Raman, and S.W. Chang, 1992: Special Sensor Microwave/Imager (SSM/I) observations of Hurricane Hugo (1989). *Mon. Wea. Rev.*, **120**, 2723-2737.

AMS, 1993: Policy Statement. Hurricane detection, tracking and forecasting. *Bull. Amer. Meteor. Soc.*, **74** (7), 1377-1380.

Anthes, R.A., 1974: The dynamics and energetics of mature tropical cyclones. *Rev. Geophys. Space Phys.*, **12** (3), 495-522.

Atlas, D., and O.W. Thiele, 1981: *Precipitation Measurements from Space*. Workshop Report, 28 April-1 May 1981, NASA GSFC, Greenbelt, MD.

Avila, L.A., and E.N. Rappaport, 1996: Eastern Pacific hurricanes. Weather of 1995. *Weatherwise*, **49** (1), 42-43.

-----, and M. Mayfield, 1995: Eastern North Pacific hurricane season of 1993. *Mon. Wea. Rev.*, **123**, 897-906.

Barbor, K., 1997: *Impact of the 1996 Hurricane Season on Atlantic Fleet Operations.*

Presentation at the 51st Interdepartmental Hurricane Conference, 25-28 March 1997, Miami, FL, OFCM.

Barrett, E.C., and M.J. Beaumont, 1994: Satellite rainfall monitoring: An overview. *Remote Sensing Reviews*, **11**, 23-48.

Bauer, P., and N.C. Grody, 1995: The potential of combining SSM/I and SSM/T2 measurements to improve the identification of snow cover and precipitation. *IEEE Trans. Geosci. Remote Sens.*, **33** (2), 252-261.

Cecil, D.J., 1997: Basin to basin differences in the relationship between ice scattering signature and future tropical cyclone intensity. *Preprints, 22nd Conf. on Hurr. and Trop. Meteor.*, 19-23 May 1997, Fort Collins, CO, Amer. Meteor. Soc., 3a.4, 31-32.

Colton, M.C., G.A. Poe, E.A. Uliana, R.W. Conway, and B. Gardiner, 1996: Intersensor calibration of DMSP SSM/I'S F8 - F13, 1987-1995. *Preprints, 8th Conf. on Sat. Meteor. and Oceanogr.*, 28 January-2 February 1996, Atlanta, GA, Amer. Meteor. Soc., 185-187.

-----, and -----, 1994: Meeting Review. Shared Processing Program, Defense Meteorological Satellite Program, Special Sensor Microwave/Imager Algorithm Symposium, 8-10 June 1993. *Bull. Amer. Meteor. Soc.*, **75** (9), 1663-1669.

Davis, M.A.S., G.M. Brown, and P.W. Leftwich, 1984: *A Tropical Cyclone Data Tape for the Eastern and Central North Pacific Basins, 1949-1983: Contents, Limitations and Uses*. NOAA Technical Memorandum NWS NHC 25. National Hurricane Center, Miami, FL, 16 pp.

DeMaria, M., and J. Kaplan, 1994: A statistical hurricane intensity prediction system (SHIPS) for the Atlantic basin. *Wea. Forecasting*, **9**, 209-220.

Dvorak, V.F., 1990: *A Workbook on Tropical Clouds and Cloud Systems Observed in Satellite Imagery, Volume II.* NAVEDTRA 40971. US Navy, Stennis Space Center, MS.

Elsberry, R.L., G.J. Holland, H. Gerrish, M. DeMaria, C.P. Guard, and K. Emanuel, 1992: Is there any hope for tropical cyclone intensity prediction?--A panel discussion. *Bull. Amer. Soc.*, **73** (3), 264-275.

Felde, G.W., and M. Glass, 1991: SSM/I brightness temperature analysis of tropical cyclones. *Preprints, 19th Conf. on Hurr. and Trop. Meteor.*, 6-10 May 1991, Miami, FL, Amer. Meteor. Soc., 400-404.

Ferraro, R.R., F. Weng, N.C. Grody, and A. Basist, 1996: An eight year (1987-1994) time series of rainfall, clouds, water vapor, snow cover, and sea ice derived from SSM/I measurements. *Bull. Amer. Soc.*, **77** (5), 891-905.

-----, and G.F. Marks, 1995: The development of SSM/I rain-rate retrieval algorithms using ground-based radar measurements. *J. Atmos. Oceanic Technol.*, **12**, 755-770.

-----, N.C. Grody, and G.F. Marks, 1994: Effects of surface conditions on rain identification using the SSM/I. *Remote Sensing Reviews*, **11**, 195-209.

Frank, N.L., and C.L. Jordan, 1960: Climatological Aspects of the Intensity of Typhoons. *Geophys. Mag.*, **30** (1), 131-148.

Gaby, D.C., J.B. Lushine, B.M. Mayfield, S.C. Pearce, and F.E. Torres, 1980: Satellite

classifications of Atlantic tropical and subtropical cyclones: A review of eight years of classifications at Miami. *Mon. Wea. Rev.*, **108**, 587-595.

Glahn, H.R., 1985: Chapter 8. Statistical weather forecasting. *Probability, Statistics, and Decision Making in the Atmospheric Sciences*. Eds. A.H. Murphy, and R.W. Katz. Westview Press, Boulder, CO. 289-335.

Glass, M., and G. W. Felde, 1992: Intensity estimation of tropical cyclones using SSM/I brightness temperatures. *Preprints, Joint Session of the Sympos. on Wea. Forecasting and 6th Conf. on Sat. Meteor. and Oceanogr.*, 5-10 January, 1992, Atlanta, GA, Amer. Meteor. Soc., J8-J10.

-----, and -----, 1990: Tropical storm structure analysis using SSM/I and OLS data. *Preprints, 5th Conf. on Sat. Meteor. and Oceanogr.*, 3-7 September 1990, London, England, Amer. Meteor. Soc., 432-437.

-----, and -----, 1989: Structure of tropical cyclones and surrounding regions as determined from OLS and SSM/I imagery analysis. *Preprints, 4th Conf. on Sat. Meteor. and Oceanogr.*, 16-19 May 1989, San Diego, CA, Amer. Meteor. Soc., 35-38.

Gray, W.M., 1968: Global view of the origin of tropical disturbances and storms. *Mon. Wea. Rev.*, **96** (10), 669-700.

Grody, N.C., 1997: Remote sensing from satellites using microwave radiometry. *Short Course on Passive Microwave Satellite Radiometry*, 2 February 1997, Long Beach, CA, Amer. Meteor. Soc.

-----, 1991: Classification of snow cover and precipitation using the Special Sensor

Microwave/Imager (SSM/I). *J. Geophys. Res.*, **96**, 7423-7435.

Gross, J.M., and M.B. Lawrence, 1996: 1995 National Hurricane Center forecast verification. *Minutes of the 50th Interdepartmental Hurricane Conference*, 26-29 March 1996, Miami, FL, OFCM, B10-B50.

Hawkins, J.D., 1997: Personal communication. Electronic mail message (hawkins@nrlmry.navy.mil), 1 May 1997. Naval Research Laboratory, Marine Meteorology Division, Monterey, CA.

-----, J. Sandidge, R. Holyer, D.A. May, G. Poe, 1996: Tropical cyclone characterization via satellite remotely sensed techniques. *Preprints, 8th Conf. on Sat. Meteor. and Oceanogr.*, 28 January-2 February 1996, Atlanta, GA, Amer. Meteor. Soc., 200-203.

Helveston, M.J., J.D. Hawkins, D.A. May, G.A. Poe, and G. Sandlin, 1996: Processing system for tropical cyclone multi-sensor satellite data sets. *Preprints, 12th International Conf. on IIPS for Meteor., Oceanogr., and Hydrology*, 28 January-2 February, 1996, Atlanta, GA, Amer. Meteor. Soc., 476-478.

Hobgood, J.S., 1997: The effects of climatological factors on the intensities of tropical cyclones over the eastern North Pacific Ocean. *Preprints, 22nd Conf. on Hurr. and Trop. Meteor.*, 19-23 May 1997, Fort Collins, CO, Amer. Meteor. Soc., 8a.4, 282-283.

-----, 1986: A possible mechanism for the diurnal oscillations of tropical cyclones. *J. Atmos. Sci.*, **43** (23), 2901-2922.

Holland, G.J., 1993: Chapter 9. Ready reckoner. *Global Guide to Tropical Cyclone*

Forecasting. World Meteorological Organization Technical Document Number 560, Tropical Cyclone Program Report Number 31, Geneva, Switzerland.

Hollinger, J.P., 1991: *DMSP Special Sensor Microwave/Imager Calibration/Validation*. Final Report Volume II, Naval Research Laboratory, Washington, DC.

-----, J.L. Peirce, and G.A. Poe, 1990: SSM/I instrument evaluation. *IEEE Trans. Geosci. Remote Sens.*, **28** (5), 781-790.

-----, 1989: *DMSP Special Sensor Microwave/Imager Calibration/Validation*. Final Report Volume I, Naval Research Laboratory, Washington, DC.

Houze, R.A., 1993: *Cloud Dynamics*. Academic Press. 573 pp.

Hughes, L.A., 1952: On the low-level wind structure of tropical storms. *J. Meteor.*, **9**, 422-428.

Hunter, H.E., E.B. Rodgers, and W.E. Shenk, 1981: An objective method for forecasting tropical cyclone intensity using Nimbus-5 Electrically Scanning Microwave Radiometer measurements. *J. Appl. Meteor.*, **20**, 137-145.

Jarvinen, B.R., and C.J. Neumann, 1979: *Statistical Forecasts of Tropical Cyclone Intensity for the North Atlantic Basin*. NOAA Technical Memorandum NWS NHC 10. National Hurricane Center, Miami, FL, 22 pp.

Johnson, R.H., and P.J. Hamilton, 1988: The relationship of surface features to the precipitation and air flow structure of an intense midlatitude squall line. *Mon. Wea. Rev.*, **116**, 1444-1472.

Jorgensen, D.P., 1984: Mesoscale and convective-scale characteristics of mature hurricanes. Part I: General observations by research aircraft. *J. Atmos. Sci.*, **41** (8),

1268-1285.

Kaplan, J., 1992: Computer subroutine ALAND written in FORTRAN 77 code.

Khrgian, A.K., 1959: *Meteorology: A Historical Survey*, Volume 1, 2nd Edition, Revised. Edited by K.P. Pogosyan, Translated from Russian by R. Hardin in 1970. Keter Press, Jerusalem, 387 pp.

Kidder, S.Q., and T.H. Vonder Haar, 1995: *Satellite Meteorology: An Introduction.* Academic Press, San Diego, CA. 466 pp.

Kurihara, Y., and R.E. Tuleya, 1974: Structure of a tropical cyclone developed in a three-dimensional numerical simulation model. *J. Atmos. Sci.*, **31**, 893-919.

Lawrence, M.B., and E.N. Rappaport, 1994: Eastern North Pacific hurricane season of 1992. *Mon. Wea. Rev.*, **122**, 549-558.

MacArthur, P.D., 1991: *Microwave Derived Rainrates in Typhoons and Their Use in the Diagnosis and Prediction of Typhoon Intensity*. Master's Thesis, Saint Louis University, 70 pp.

Marks, F.D., 1990: Radar observations of tropical weather systems. *Radar in Meteorology: Battan Memorial and 40th Anniversary Radar Meteorology Conference*, Boston, MA, Amer. Meteor. Soc., 401-425.

Martin, J.D., and W.M. Gray, 1993: Tropical cyclone observation and forecasting with and without aircraft reconnaissance. *Wea. Forecasting*, **8**, 519-532.

McBride, J.L., 1995: Chapter 3. Tropical cyclone formation. *Global Perspectives on Tropical Cyclones*. World Meteorological Organization Technical Document Number 693, Tropical Cyclone Program Report Number 38, Geneva, Switzerland.

McCoy, J.H., 1991: *Tropical Cyclone Asymmetries as Revealed by Recent Satellite Brightness Temperatures*. Master's Thesis, Saint Louis University, 133 pp.

Melton, E.C., 1994: *Analysis of the Structural Characteristics and Intensity Evolution of Super Typhoon Flo (1990) in Special Sensor Microwave/Imager (SSM/I) Data.* Master's Thesis, North Carolina State University, 112 pp.

Merrill, R.T., 1987: *An Experiment in Statistical Prediction of Tropical Cyclone Intensity Change*. NOAA Technical Memorandum NWS NHC 34. National Hurricane Center, Miami, FL, 34 pp.

Middleton, W.E.K., 1965: *A History of the Theories of Rain and Other Forms of Precipitation*. Franklin Watts, Incorporated, New York, NY. 223 pp.

Miller, D., 1997: Personal communication. Electronic mail message (miller@npmocw.navy.mil), 7 May 1997. TSgt, USAF, Joint Typhoon Warning Center, Nimitz Hill, Guam.

Molinari, J., D. Vollaro, and F. Robasky, 1992: Use of ECMWF operational analyses for studies of the tropical environment. *Meteor. Atmos. Phys.*, **47**, 127-144.

Mundell, D.B., 1991: Tropical cyclone intensification. *Preprints, 19th Conf. on Hurr. and Trop. Meteor.*, May 6-10, 1991, Miami, FL, Amer. Meteor. Soc., 511-515.

-----, 1990: *Prediction of Tropical Cyclone Rapid Intensification Events*. Master's Thesis, Colorado State University, 186 pp.

Neumann, C.J., 1993: Chapter 1. Global overview. *Global Guide to Tropical Cyclone Forecasting*. World Meteorological Organization Technical Document Number 560, Tropical Cyclone Program Report Number 31, Geneva, Switzerland.

OFCM, 1997: *National Plan for Tropical Cyclone Research and Reconnaissance (1997-2002)*. Office of the Federal Coordinator for Meteorological Services and Supporting Research, FCM-P25-1997, Washington, DC.

-----, 1996: *National Hurricane Operations Plan.* Office of the Federal Coordinator for Meteorological Services and Supporting Research, FCM-P12-1996, Washington, DC.

Palmén, E., 1948: On the formation and structure of tropical hurricanes. *Geophysica*, **3**, 26-38.

Pasch, R.J., and M. Mayfield, 1996: Eastern North Pacific hurricane season of 1994. *Mon. Wea. Rev.*, **124**, 1579-1590.

Petty, K.R., 1997: The effects of synoptic factors on the intensities of tropical cyclones over the eastern North Pacific Ocean. *Preprints, 22nd Conf. on Hurr. and Trop. Meteor.*, 19-23 May 1997, Fort Collins, CO, Amer. Meteor. Soc., 8a.2, 278-279.

Poe, G.A., 1997: Review of satellites-Historical perspective. *Short Course on Passive Microwave Satellite Radiometry*, 2 February 1997, Long Beach, CA, Amer. Meteor. Soc.

Rao, G.V., and P.D. MacArthur, 1994: The SSM/I estimated rainfall amounts of tropical cyclones and their potential in predicting the cyclone intensity changes. *Mon. Wea. Rev.*, **122**, 1568-1574.

-----, -----, and J.H. McCoy, 1991: The latent heat release and brightness temperature anomalies associated with tropical cyclones and their utility in predicting the intensity changes of tropical storms. *Preprints, 19th Conf. on Hurr. and Trop.*

Meteor., 6-10 May 1991, Miami, FL, Amer. Meteor. Soc., 175-178.

Rao, K.P., S.J. Holmes, R.K. Anderson, J.S. Winston, P.E. Lehr, 1990: *Weather Satellites: Systems, Data, and Environmental Applications*. Amer. Meteor. Soc., Boston, MA.

Rappaport, E.N., and M. Mayfield, 1997: Eastern Pacific hurricane season: A quiet year. 1996 U.S. highlights. *Weatherwise*, **50** (1), 42-43.

-----, 1991: *Preprints, 19th Conf. on Hurr. and Trop. Meteor.*, 6-10 May 1991, Miami, FL, Amer. Meteor. Soc.

Reynolds, R.W., and T.M. Smith, 1994: Improved global sea surface temperature analyses using optimal interpolation. *J. Climate*, **7**, 929-948.

Rhudy, D.K., 1989: *Applications of Microwave Radiometric Measurements to Infer Tropical Cyclone Intensity and Strength.* Master's Thesis, Saint Louis University, 91 pp.

Riehl, H., 1954: *Tropical Meteorology*. McGraw-Hill Book Company, New York. 392 pp.

Rodgers, E.B., W.S. Olson, V.M. Karyampudi, and H.F. Pierce, 1997: The response of Opal's (1995) intensity to its satellite observed latent heat distribution. *Preprints, 22nd Conf. on Hurr. and Trop. Meteor.*, 19-23 May 1997, Fort Collins, CO, Amer. Meteor. Soc., 3a.3, 29-30.

-----, and H.F. Pierce, 1995a: A satellite observational study of precipitation characteristics in western North Pacific tropical cyclones. *J. Appl. Meteor.*, **34**, 2587-2599.

-----, and -----, 1995b: Environmental influence on Typhoon Bobbie's precipitation distribution. *J. Appl. Meteor.*, **34**, 2513-2532.

-----, J.-J. Baik, and H.F. Pierce, 1994a: The environmental influence on tropical cyclone precipitation. *J. Appl. Meteor.*, **33**, 573-593.

-----, S.W. Chang, and -----, 1994b: A satellite observational and numerical study of precipitation characteristics in western North Atlantic tropical cyclones. *J. Appl. Meteor.*, **33**, 129-139.

-----, and R.F. Adler, 1981: Tropical cyclone rainfall characteristics as determined from a satellite passive microwave radiometer. *Mon. Wea. Rev.*, **109** (3), 506-521.

Rosenthal, L., 1978: Numerical simulation of tropical cyclone development with latent heat release by the resolvable scales. Part 1. Model description and preliminary results. *J. Atmos. Sci.*, **35**, 258-271.

Sampson, C.R., R.A. Jeffries, J-H. Chu, and C.J. Neumann, 1995: *Tropical Cyclone Forecasters Reference Guide. 6. Tropical Cyclone Intensity.* NRL/PU/7541--95-0012. Naval Research Laboratory, Monterey, CA.

Shapiro, L.J., and H.E. Willoughby, 1982: The response of balanced hurricanes to local sources of heat and momentum. *J. Atmos. Sci.*, **39**, 378-394.

Sheets, R.C., 1990: The National Hurricane Center--Past, present and future. *Wea. Forecasting*, **5** (2), 185-232.

Simpson, R.H., and H. Riehl, 1981: *The Hurricane and Its Impact*. Louisiana State University Press, Baton Rogue, LA. 398 pp.

Skou, N., 1989: *Microwave Radiometer Systems: Design and Analysis*. Artech House,

Norwood, MA.

Spencer, R.W., H.M. Goodman, and R.E. Hood, 1989: Precipitation retrieval over land and ocean with the SSM/I: Identification and characteristics of the scattering signal. *J. Atmos. Oceanic Technol.*, **6**, 254-273.

Tai, K.-S., and Y. Ogura, 1987: An observational study of easterly waves over the eastern Pacific in the northern summer using FGGE data. *J. Atmos. Sci.*, **44** (2), 339-361.

Titley, D., 1995: Hurricane Gordon: Evasion at sea. *Minutes of the 49th Interdepartmental Hurricane Conference*, 14-17 February 1995, Miami, FL, OFCM, B73-B89.

Tokay, A., and D.A. Short, 1996: Evidence from tropical raindrop spectra of the origin of rain from stratiform versus convective clouds. *J. Appl. Meteor.*, **35**, 355-371.

US Navy, 1956: *Fourth Research Report, Task 12: Intensification of tropical cyclones Atlantic and Pacific areas*. Project AROWA, Norfolk NAS, VA.

Velden, C.S., W.S. Olson, and B.A. Roth, 1989: Tropical cyclone center-fixing using DMSP SSM/I data. *Preprints, 4th Conf. on Sat. Meteor. and Oceanogr.*, 16-19 May 1989, San Diego, CA, Amer. Meteor. Soc., J36-J39.

Weng, F., and N.C. Grody, 1994: Retrieval of cloud liquid water using the Special Sensor Microwave/Imager (SSM/I). *J. Geophys. Res.*, **99**, 25535-25551.

Wentz, F.J., 1995: *Deriving Earth Science Products from SSM/I*: Progress Report for Contract NASW-4714, August 1993 Through January 1995. Remote Sensing Systems Technical Memorandum 010395. Santa Rosa, CA.

West, D.A., 1997: The effects of rainfall on the intensity change of tropical cyclones over the eastern North Pacific Ocean. *Preprints, 22nd Conf. on Hurr. and Trop.*

Meteor., 19-23 May 1997, Fort Collins, CO, Amer. Meteor. Soc., 3a.5, 33-34.

-----, 1993a: Environmental influencing of Tropical Cyclone Freda's precipitation. *Preprints, 20th Conf. on Hurr. and Trop. Meteor.*, 10-14 May 1993, San Antonio, TX, Amer. Meteor. Soc., 181-184.

-----, 1993b: *Spatial and Temporal Variations of Satellite Microwave Measurements of Latent Heat Release in Tropical Cyclones Due to Environmental Forcing Obtained from a Numerical Model.* Master's Thesis, The Ohio State University, 115 pp.

Whitney, L.D. and J.S. Hobgood, 1997: The relationship between sea surface temperatures and maximum intensities of tropical cyclones in the eastern North Pacific Ocean. *J. Climate* (accepted for publication).

-----, 1995: *The Relationship Between Sea Surface Temperature and Maximum Intensity of Tropical Cyclones in the Eastern North Pacific Ocean.* Master's Thesis, The Ohio State University, 86 pp.

Wilheit, T., R. Adler, S. Avery, E. Barrett, P. Bauer, W. Berg, A. Chang, J. Ferriday, N. Grody, S. Goodman, C. Kidd, D. Kniveton, C. Kummerow, A. Mugnai, W. Olson, G. Petty, A. Shibata, and E. Smith, 1994: Algorithms for the retrieval of rainfall from passive microwave measurements. *Remote Sensing Reviews*, **11**, 163-194.

Willoughby, H.E., 1990: Temporal changes of the primary circulation in tropical cyclones. *J. Atmos. Sci.*, **47** (2), 242-264.

-----, 1988: The dynamics of the tropical cyclone core. *Aust. Meteor. Mag.*, **36**, 183-191.

-----, F.D. Marks, and R.J. Feinberg, 1984: Stationary and moving convective bands in hurricanes. *J. Atmos. Sci.*, **41** (22), 3189-3211.

-----, J.A. Clos, and M.G. Shoreibah, 1982: Concentric eye walls, secondary wind maxima, and the evolution of the hurricane vortex. *J. Atmos. Sci.*, **39**, 395-411.

Zehr, R.M., 1992: *Tropical Cyclogenesis in the Western North Pacific*. NOAA Technical Report NESDIS 61. Washington, DC, 181 pp.

Zhao, H., 1994: *Analysis of Tropical Cyclones Using Microwave Data from the Special Sensor Microwave/Imager*. Master's Thesis, University of Washington, 82 pp.

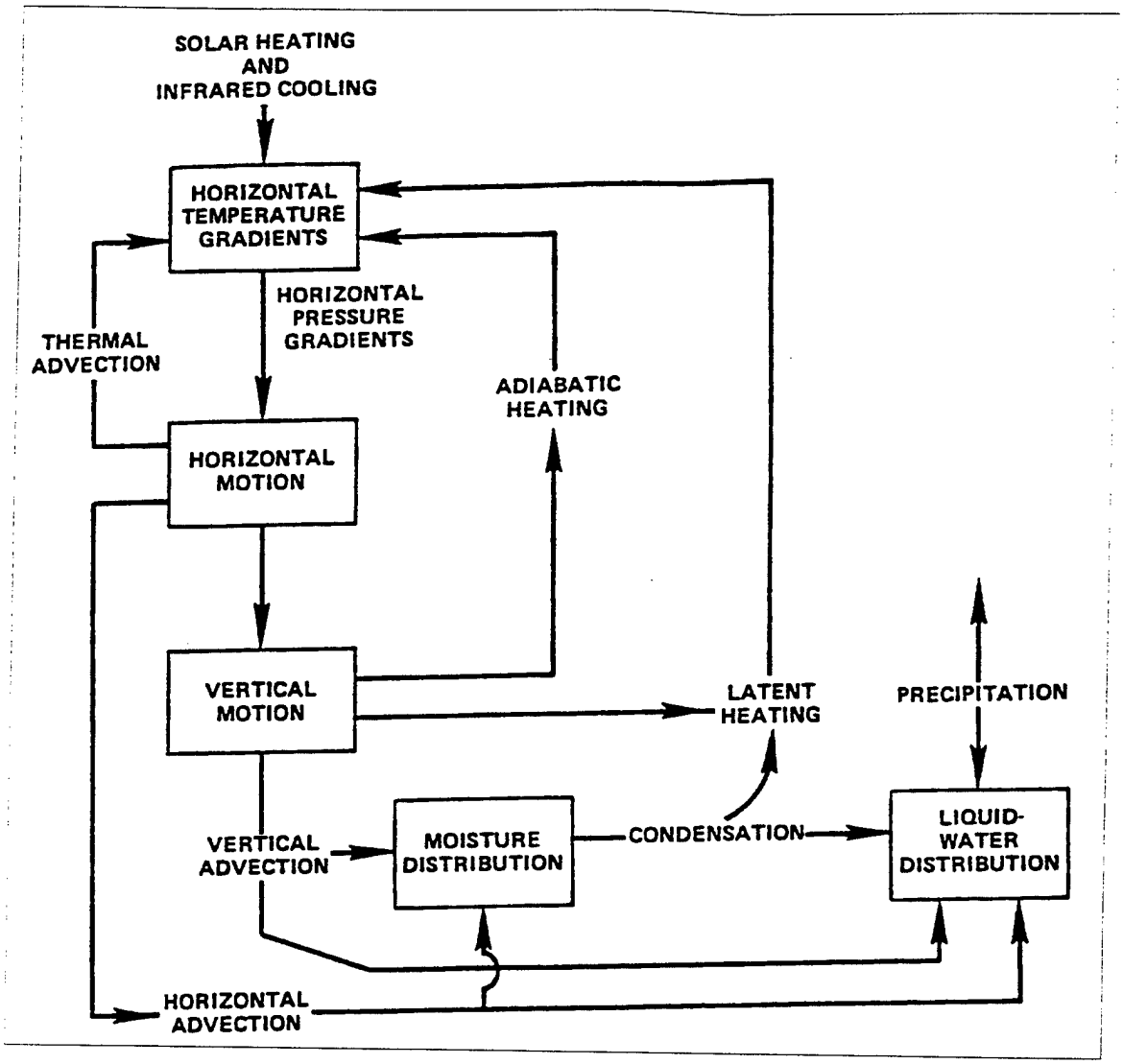

Figure 1: Interactions of synoptic-scale water and motion fields (Atlas and Thiele 1981).

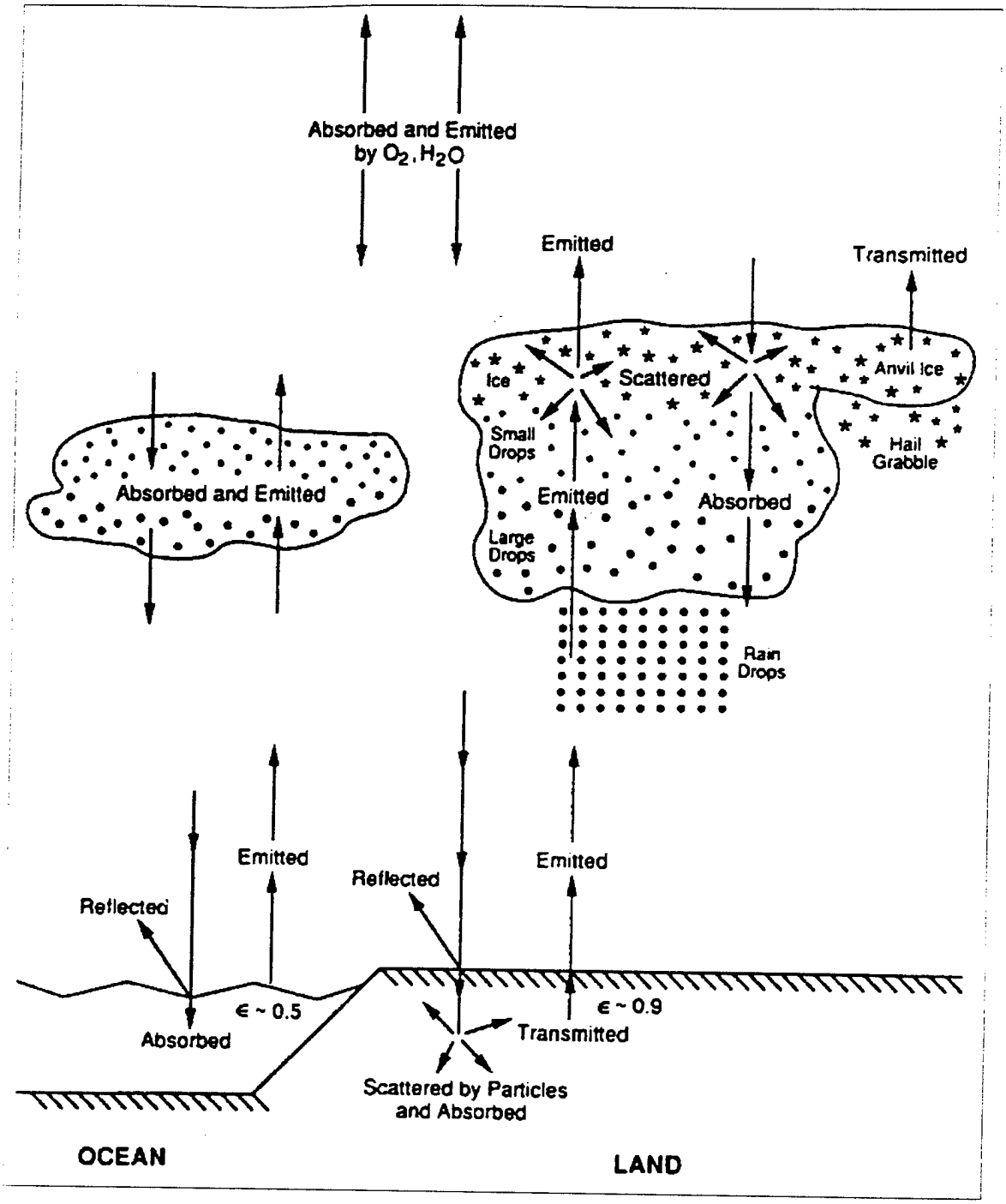

Figure 2: Interactions involving microwave radiation (Rao *et al.* 1990).

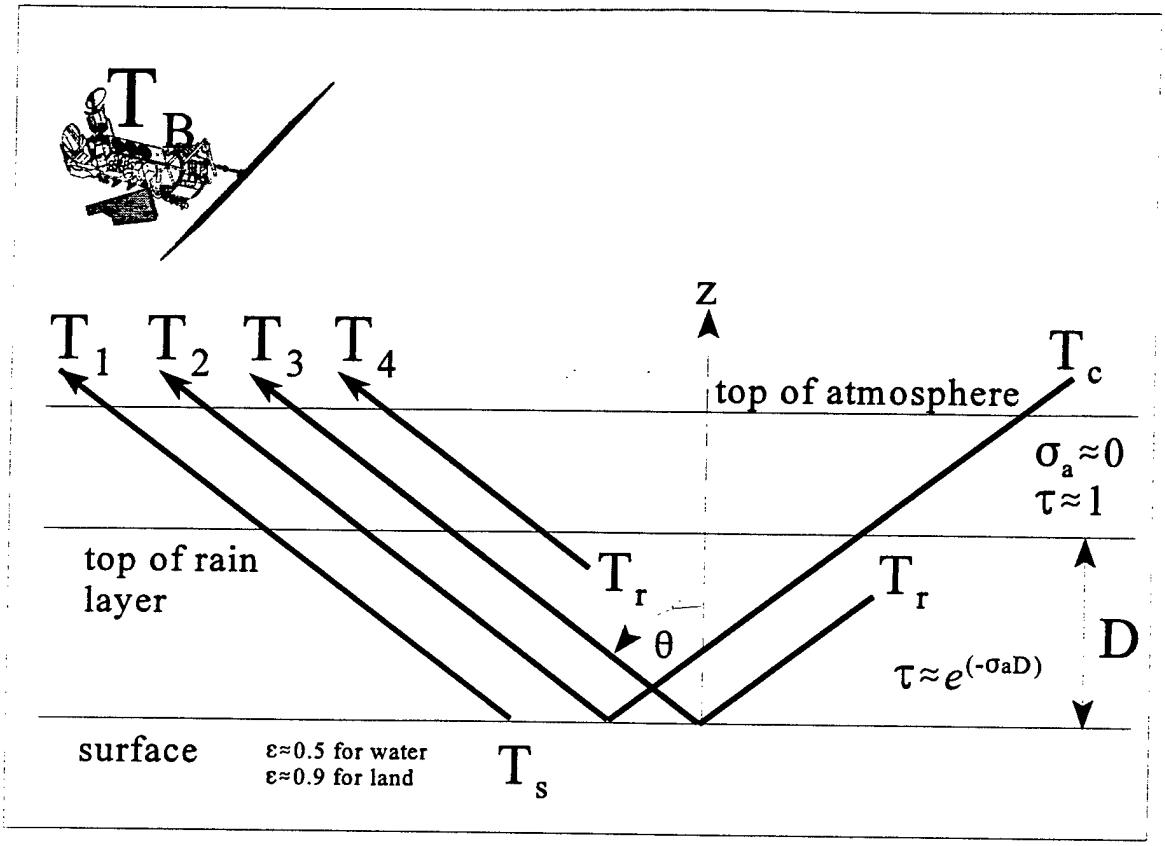

Figure 3: Geometry describing microwave radiative transfer involving rainfall.

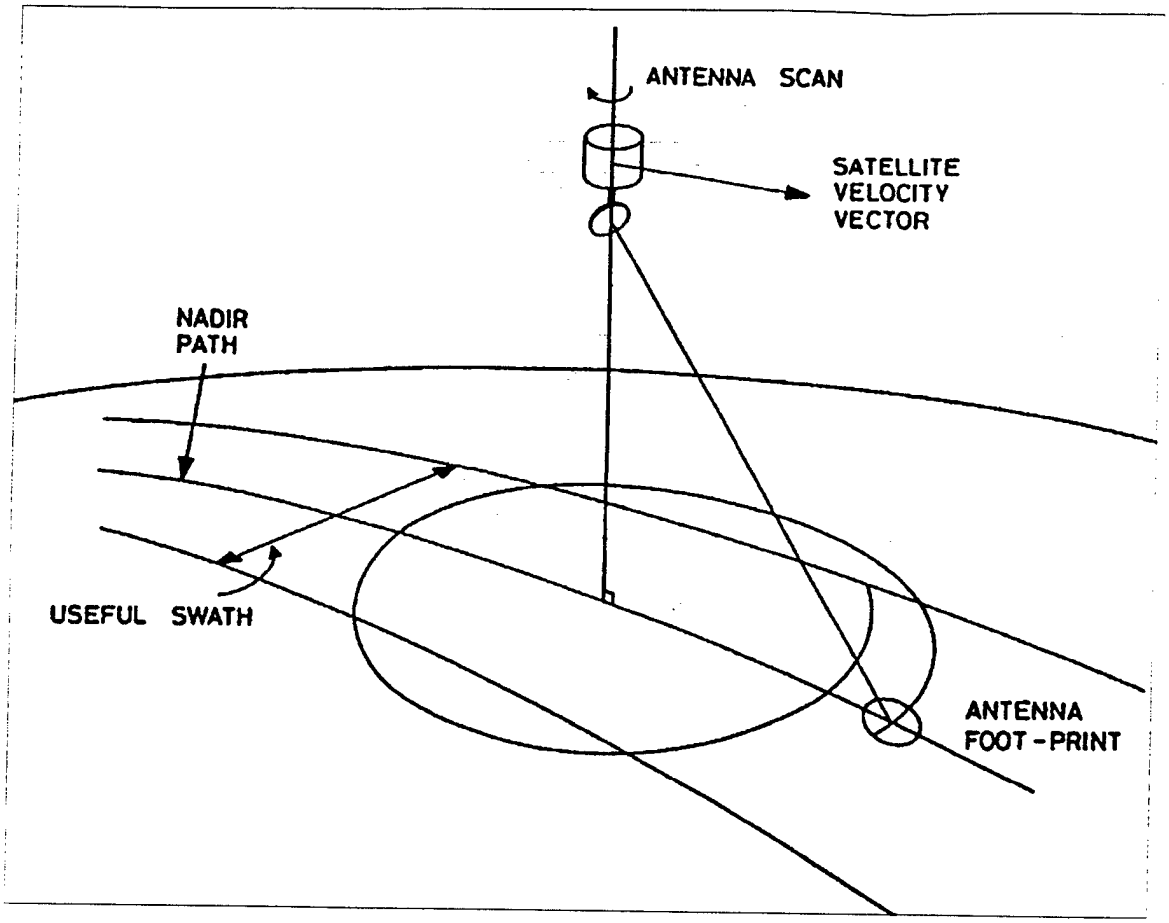

Figure 4: Conical scanning radiometer (Skou 1989).

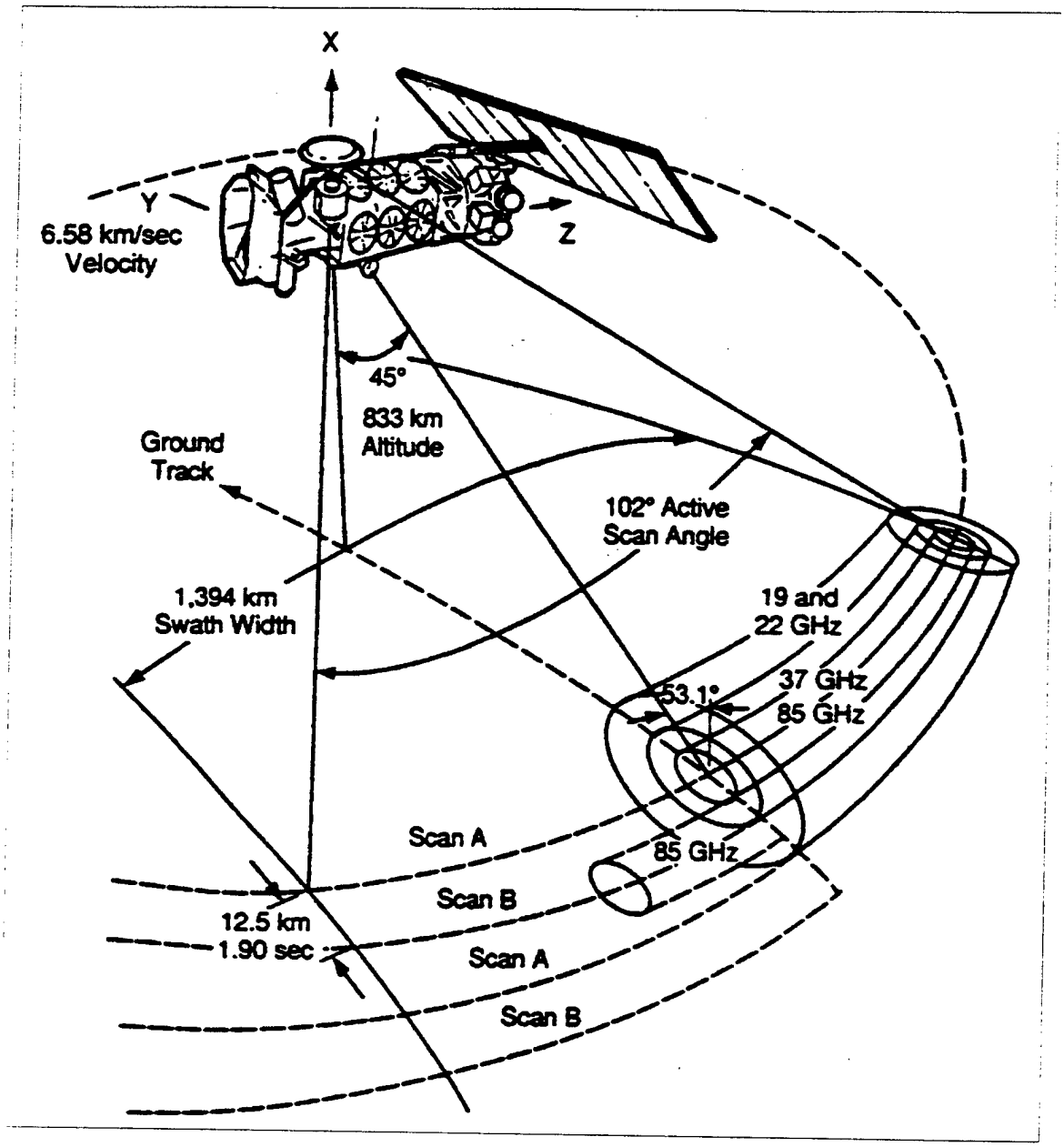

Figure 5: SSM/I scan geometry (Hollinger *et al.* 1990).

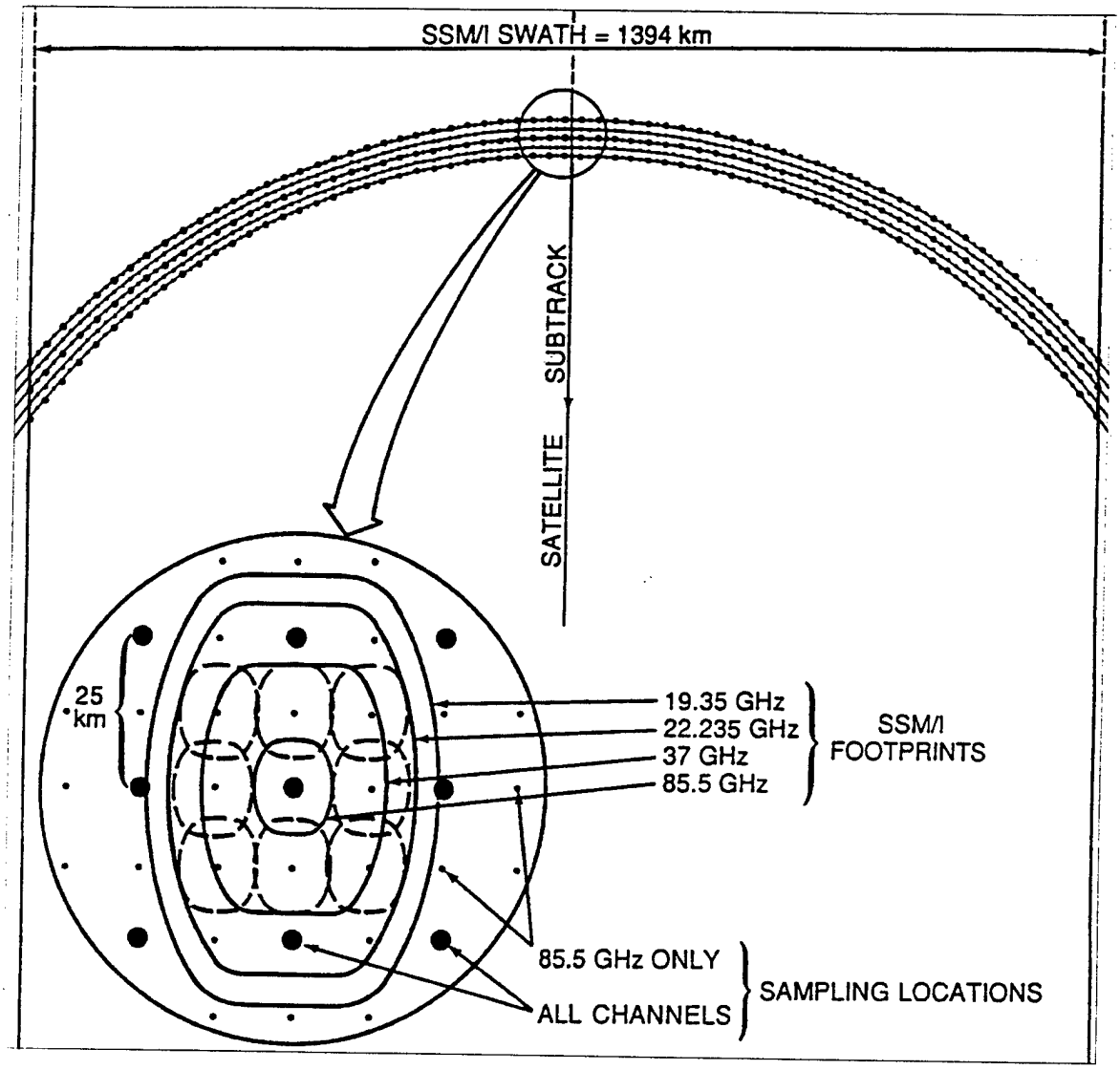

Figure 6: SSM/I scan characteristics (Spencer *et al.* 1989).

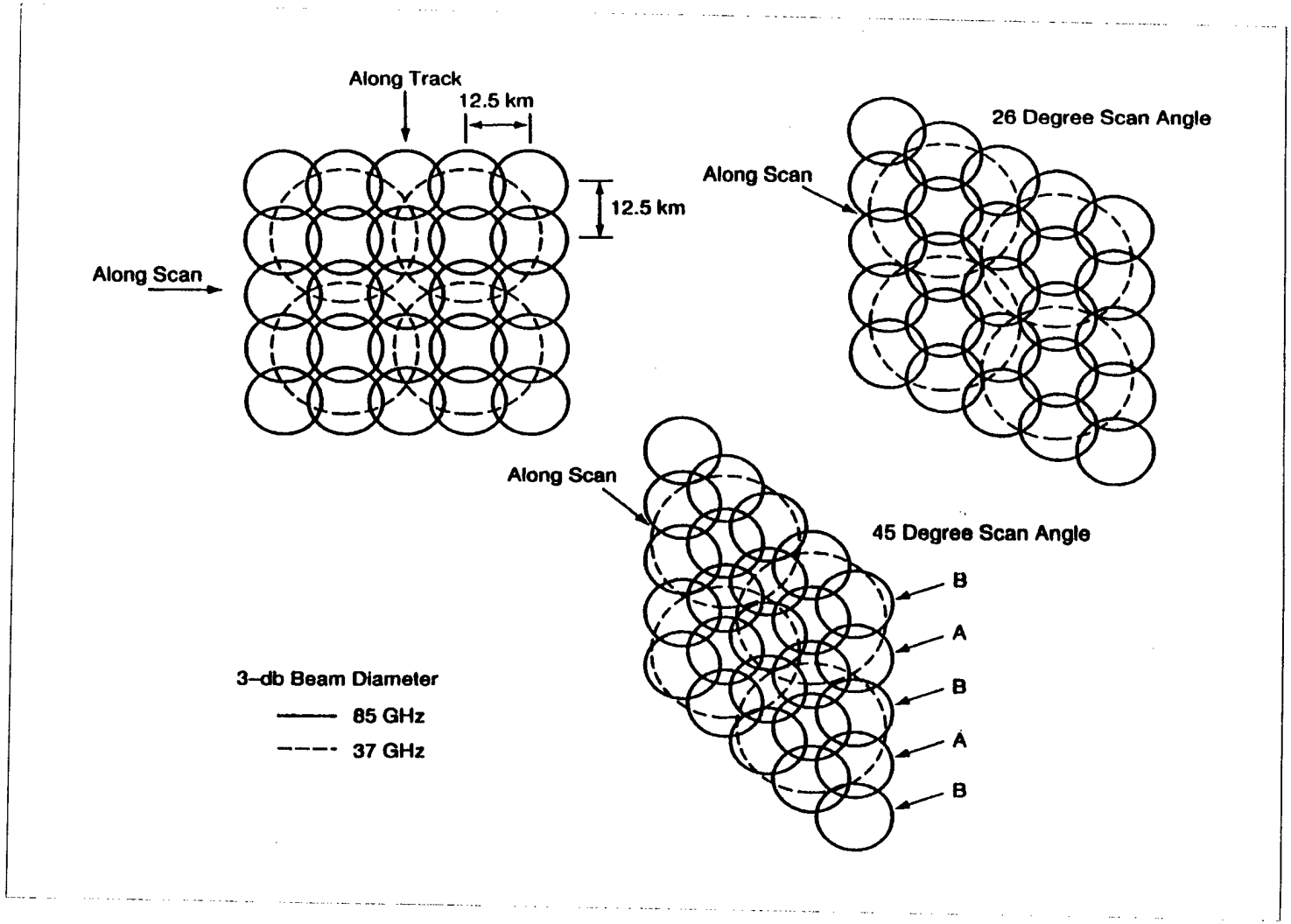

Figure 7: SSM/I spatial sampling illustrating along-scan changes (Hollinger 1989).

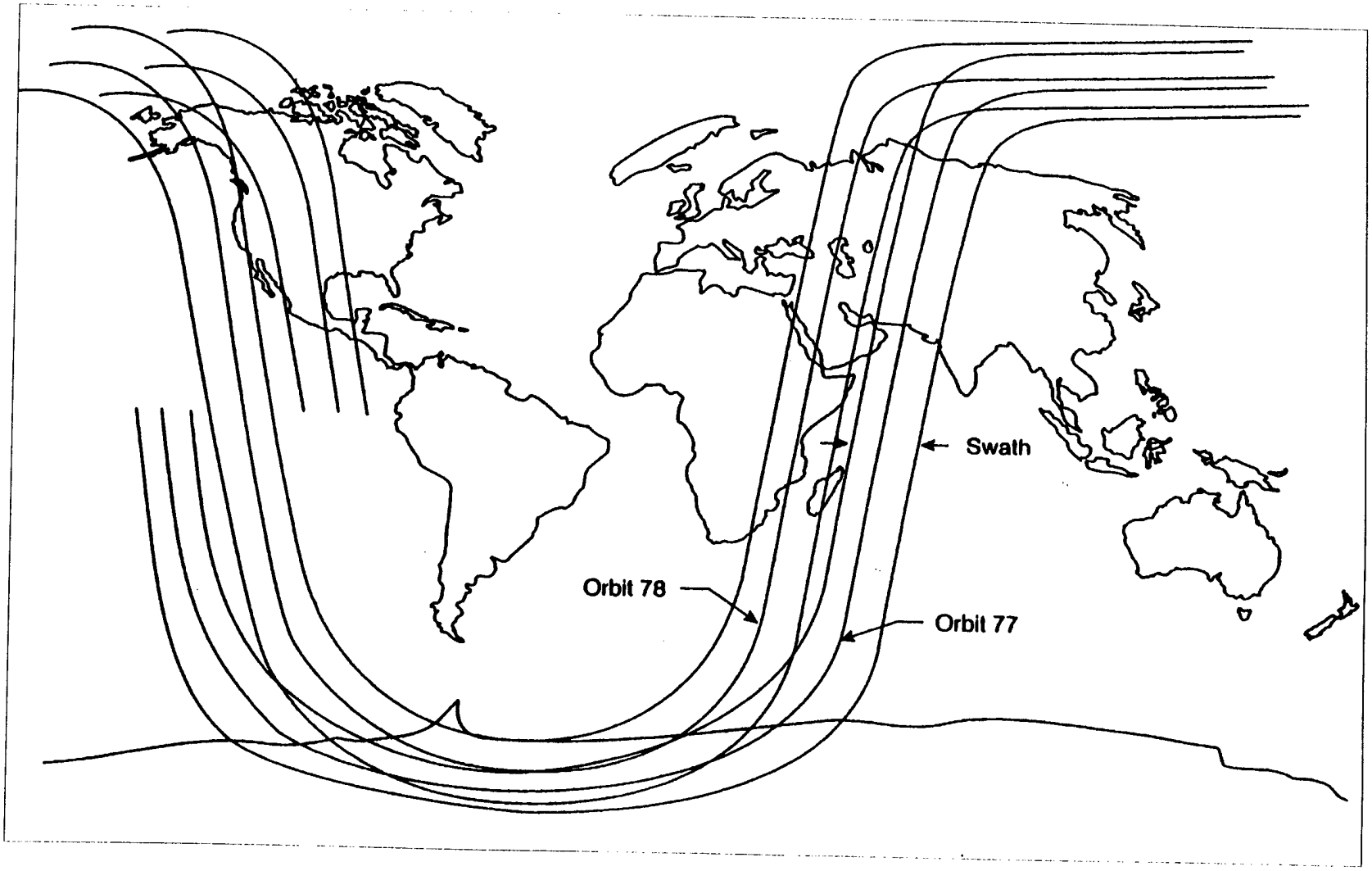

Figure 8: Equatorial view of successive SSM/I orbits with swath widths (Hollinger 1989).

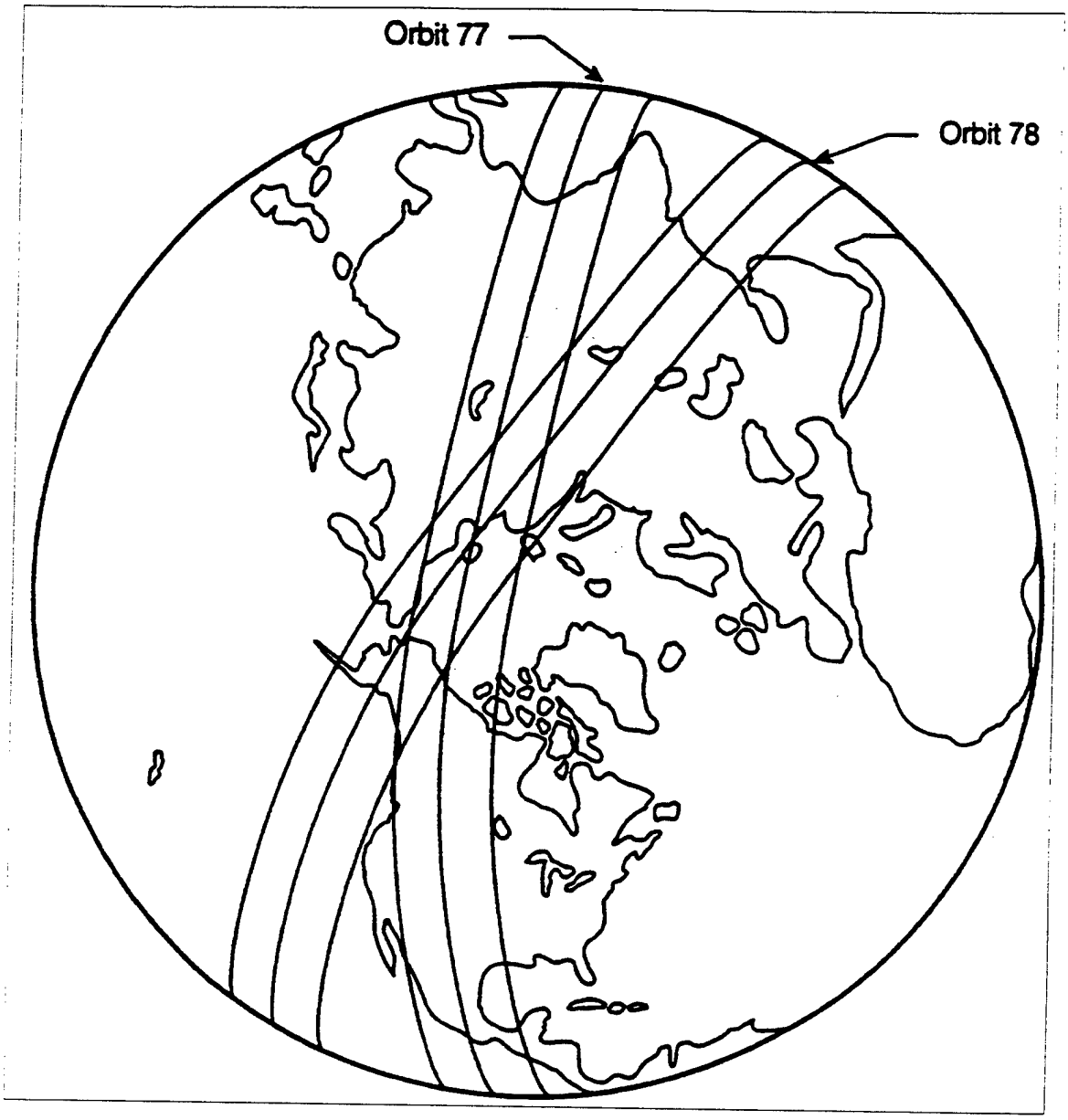

Figure 9: Polar view of successive SSM/I orbits with swath widths (Hollinger 1989).

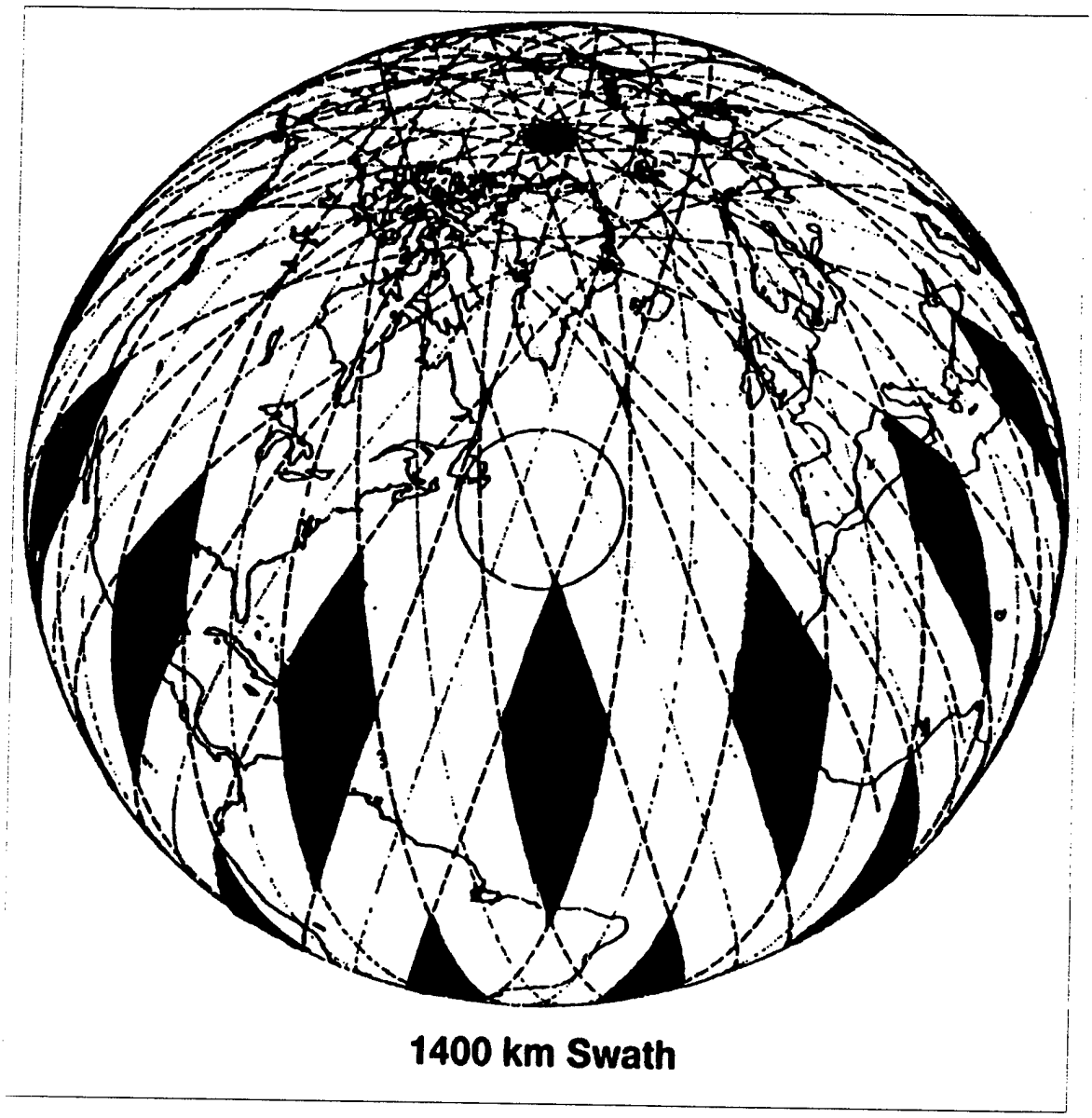

Figure 10: Coverage by one SSM/I in 24 hours. Dark areas indicate data gaps (Hollinger 1989).

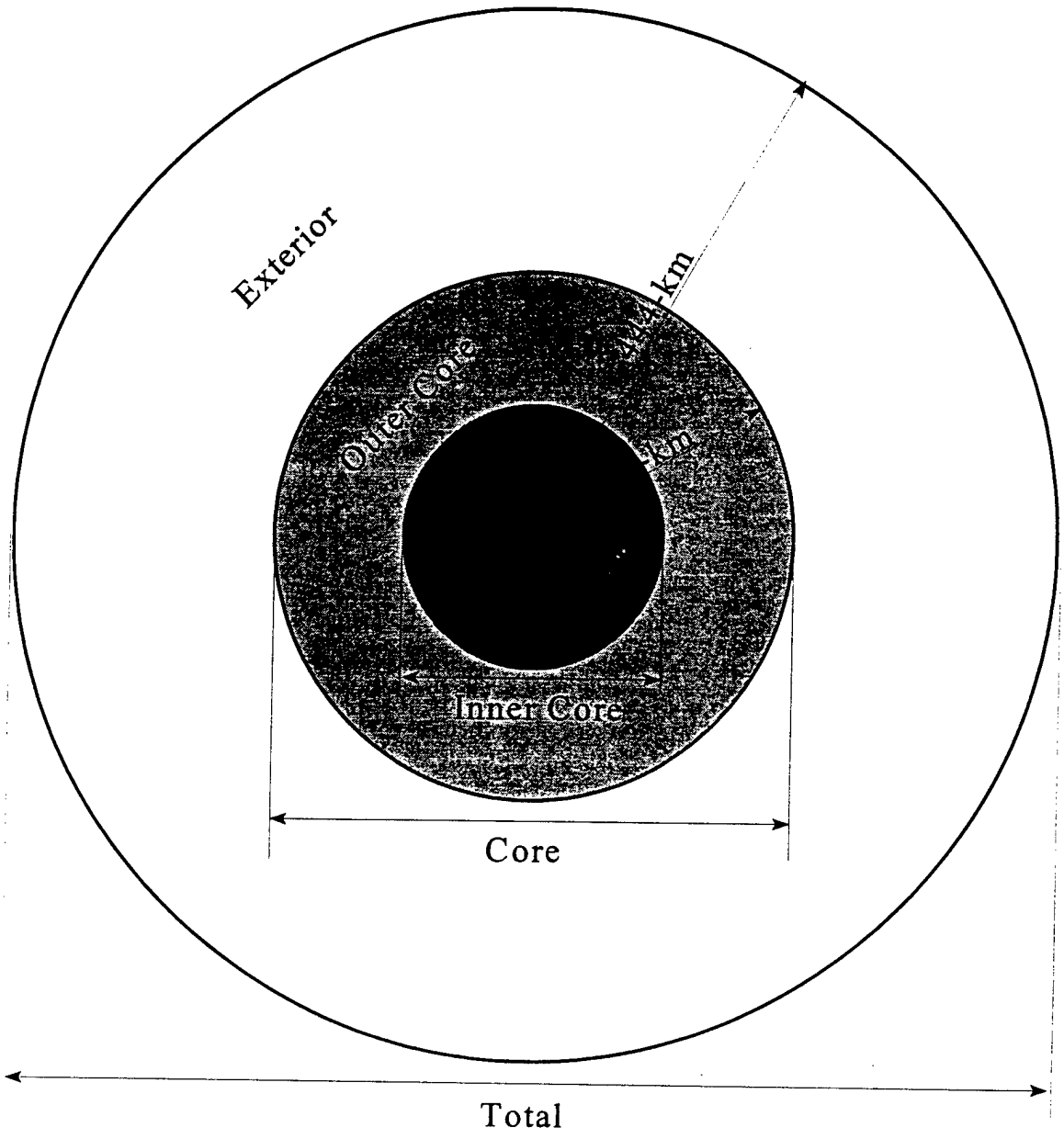

Figure 11: Circular and annular regions to be used for average rain rate calculations.

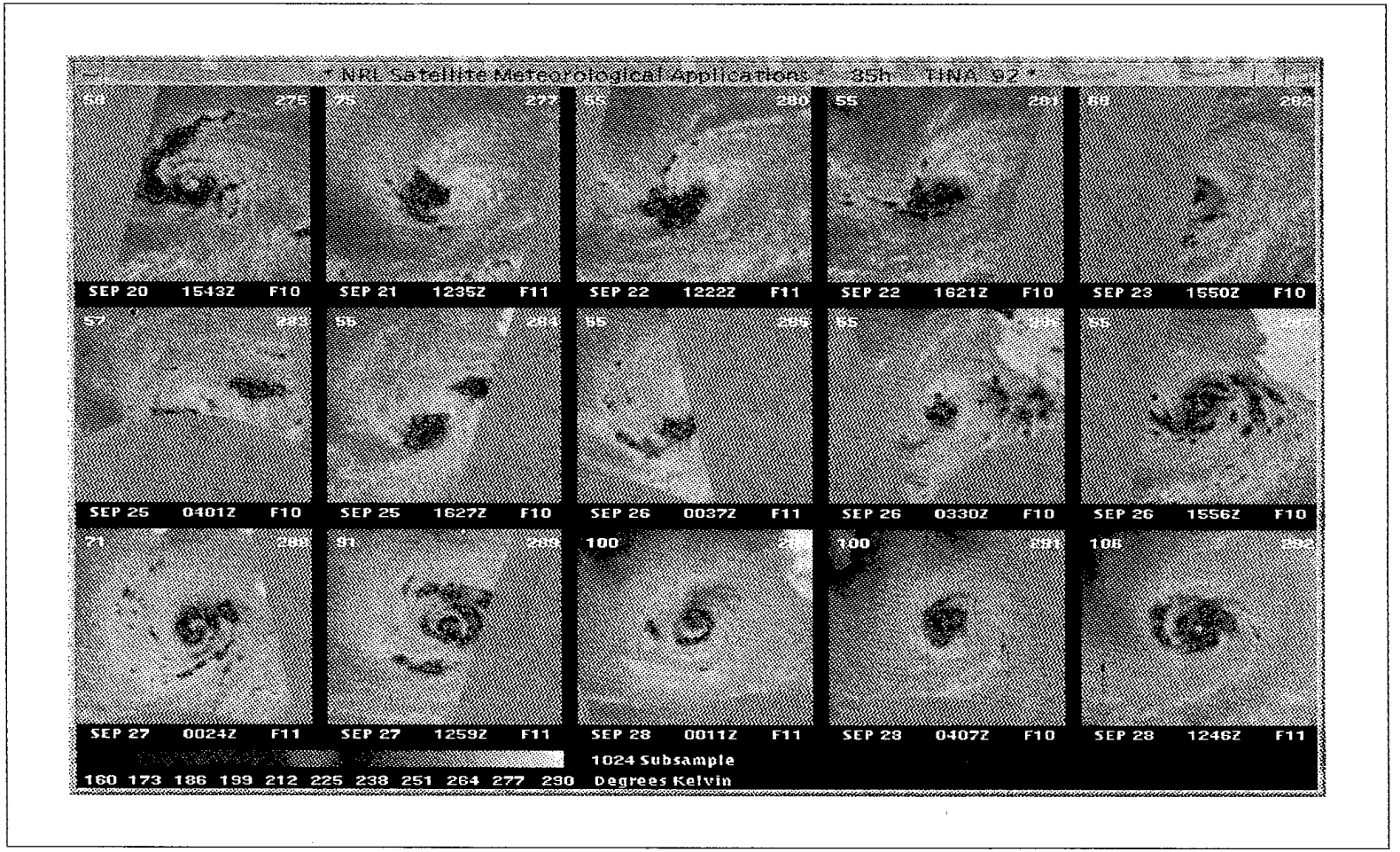

Figure 12: 15-panel 85.5 GHz horizontally polarized T_B images created by TROPX. Images depict Tropical Cyclone Tina (1992) from 20-28 September. Number in the upper-left corner of each image is interpolated best track intensity in knots. Date, time and DMSP flight number are indicated below each image.

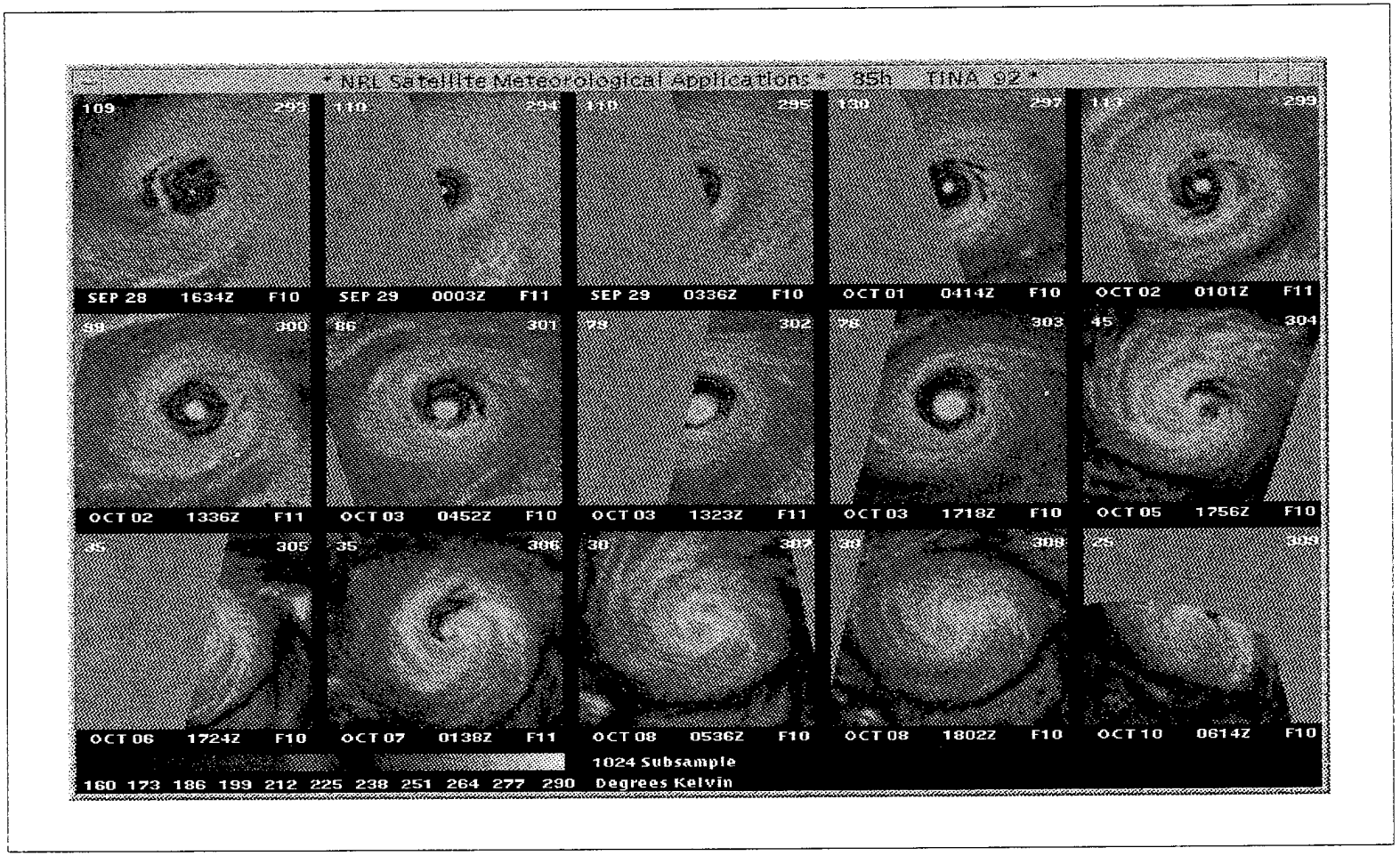

Figure 13: 15-panel 85.5 GHz horizontally polarized T_B images created by TROPX. Images depict Tropical Cyclone Tina (1992) from 28 September to 10 October. Number in the upper-left corner of each image is interpolated best track intensity in knots. Date, time and DMSP flight number are indicated below each image.

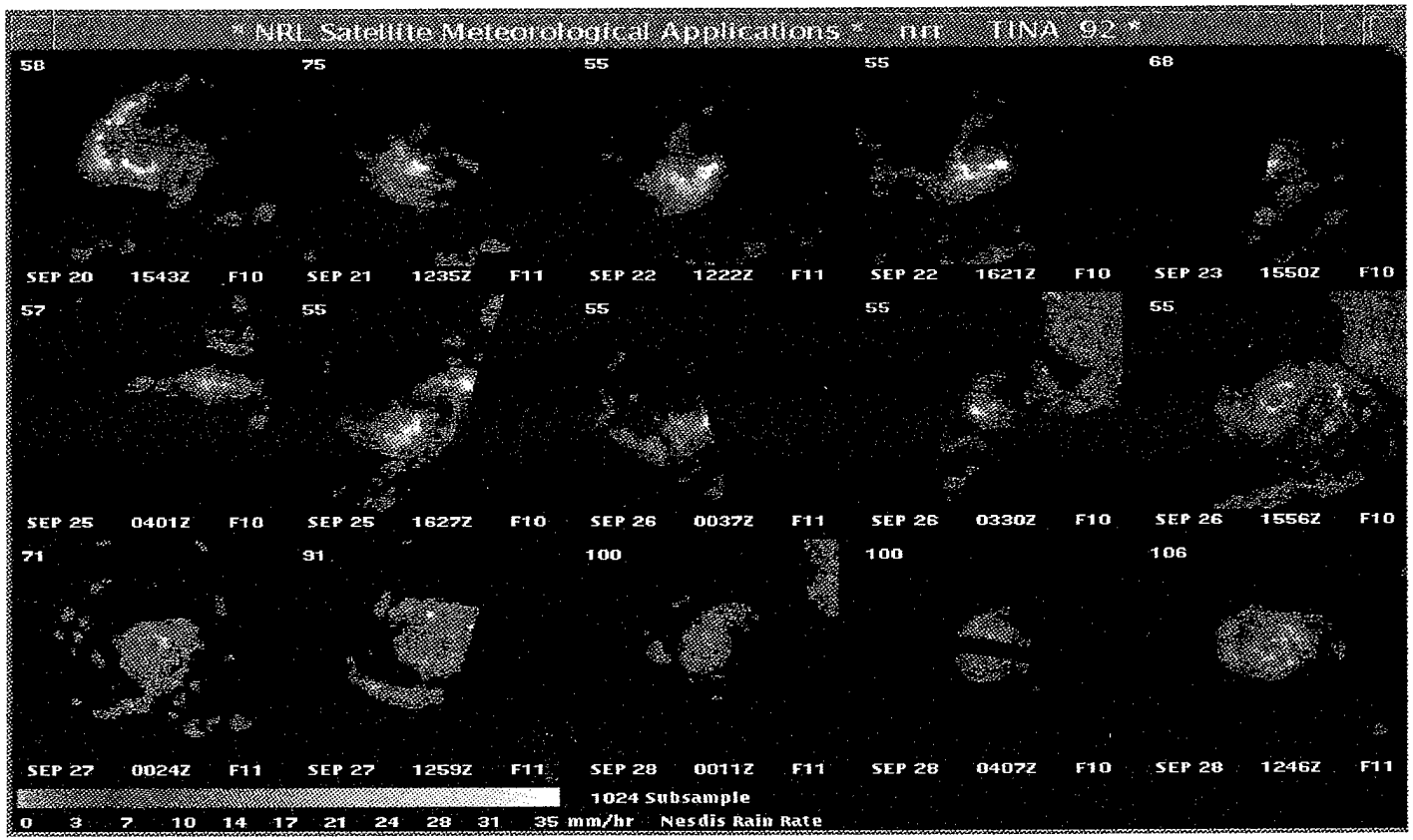

Figure 14: 15-panel NESDIS/ORA rainfall algorithm images created by TROPX. Images depict Tropical Cyclone Tina (1992) from 20-28 September. Number in the upper-left corner of each image is interpolated best track intensity in knots. Date, time and DMSP flight number are indicated below each image.

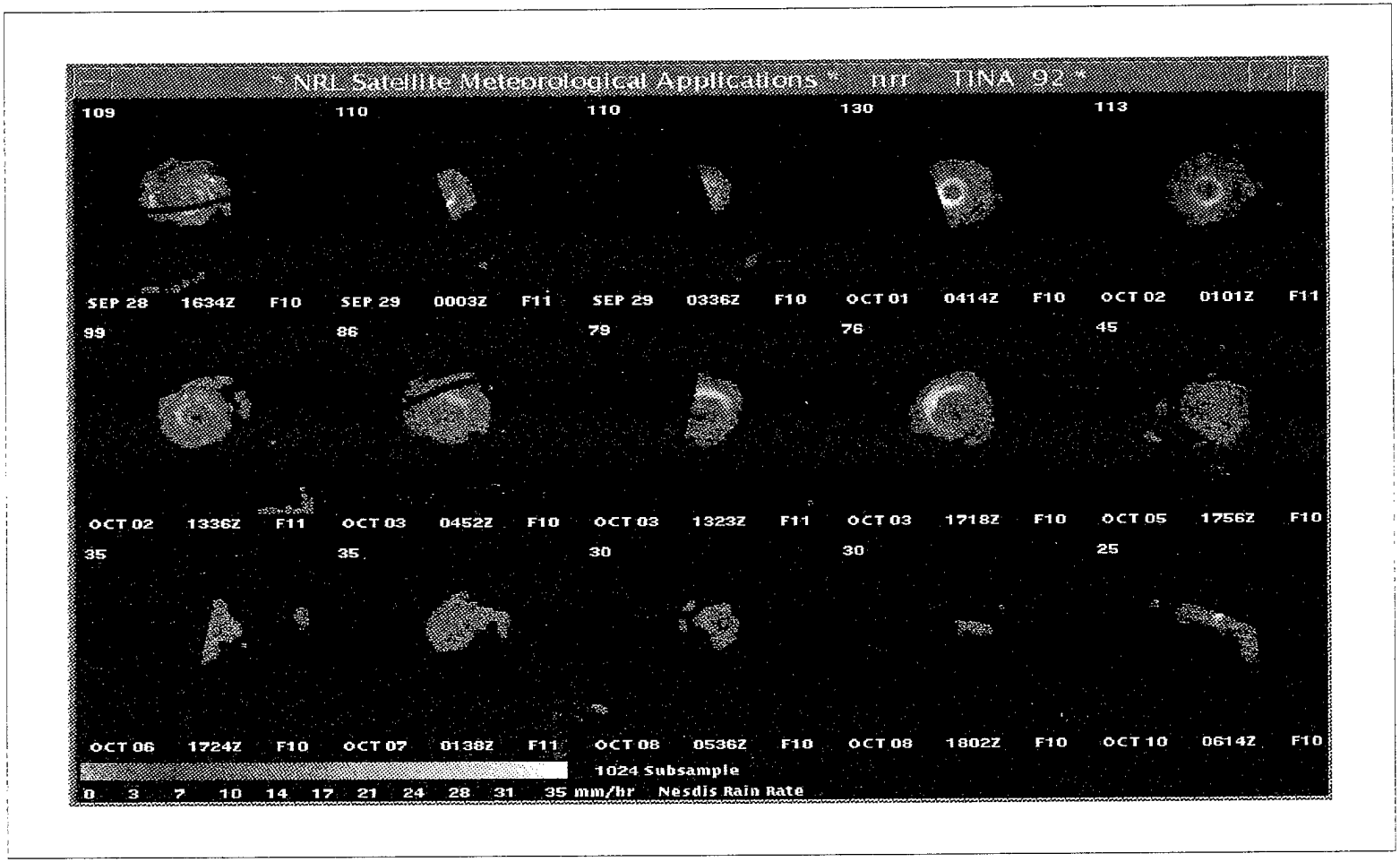

Figure 15: 15-panel NESDIS/ORA rainfall algorithm images created by TROPX. Images depict Tropical Cyclone Tina (1992) from 28 September to 10 October. Number in the upper-left corner of each image is interpolated best track intensity in knots. Date, time and DMSP flight number are indicated below each image.